

1 **Trends in secondary inorganic aerosol pollution in China and its responses to**  
2 **emission controls of precursors in wintertime**

3 Fanlei Meng<sup>1#</sup>, Yibo Zhang<sup>2#</sup>, Jiahui Kang<sup>1</sup>, Mathew R. Heal<sup>3</sup>, Stefan Reis<sup>4,3,5</sup>, Mengru  
4 Wang<sup>6</sup>, Lei Liu<sup>7</sup>, Kai Wang<sup>1</sup>, Shaocai Yu<sup>2\*</sup>, Pengfei Li<sup>8</sup>, Jing Wei<sup>9</sup>, Yong Hou<sup>1</sup>, Ying  
5 Zhang<sup>1</sup>, Xuejun Liu<sup>1</sup>, Zhenling Cui<sup>1</sup>, Wen Xu<sup>1\*</sup>, Fusuo Zhang<sup>1</sup>

6

7 <sup>1</sup>College of Resources and Environmental Sciences, National Academy of Agriculture  
8 Green Development, Key Laboratory of Plant–Soil Interactions, Ministry of Education,  
9 National Observation and Research Station of Agriculture Green Development  
10 (Quzhou, Hebei), China Agricultural University, Beijing 100193, China.

11 <sup>2</sup>Research Center for Air Pollution and Health, Key Laboratory of Environmental  
12 Remediation and Ecological Health, Ministry of Education, College of Environment  
13 and Resource Sciences, Zhejiang University, Hangzhou, Zhejiang 310058, P.R. China

14 <sup>3</sup>School of Chemistry, The University of Edinburgh, David Brewster Road, Edinburgh  
15 EH9 3FJ, United Kingdom

16 <sup>4</sup>UK Centre for Ecology & Hydrology, Penicuik, EH26 0QB, United Kingdom.

17 <sup>5</sup>University of Exeter Medical School, Knowledge Spa, Truro, TR1 3HD United  
18 Kingdom.

19 <sup>6</sup>Water Systems and Global Change Group, Wageningen University & Research, P.O.  
20 Box 47, 6700 AA Wageningen, The Netherlands

21 <sup>7</sup>College of Earth and Environmental Sciences, Lanzhou University, Lanzhou 730000,  
22 China

23 <sup>8</sup>College of Science and Technology, Hebei Agricultural University, Baoding, Hebei  
24 071000, China

25 <sup>9</sup>Department of Atmospheric and Oceanic Science, Earth System Science  
26 Interdisciplinary Center, University of Maryland, College Park 20740, USA

27

28 \*Corresponding authors

29 E-mail addresses: W. Xu ([wenxu@cau.edu.cn](mailto:wenxu@cau.edu.cn)); S C. Yu ([shaocaiyu@zju.edu.cn](mailto:shaocaiyu@zju.edu.cn))

30 # Contributed equally to this work.

31

32

33 **ABSTRACT:** The Chinese government recently proposed ammonia (NH<sub>3</sub>) emissions  
34 reductions (but without a specific national target) as a strategic option to mitigate PM<sub>2.5</sub>  
35 pollution. We combined a meta-analysis of nationwide measurements and air quality  
36 modelling to identify efficiency gains by striking a balance between controlling NH<sub>3</sub>  
37 and acid gas (SO<sub>2</sub> and NO<sub>x</sub>) emissions. We found that PM<sub>2.5</sub> concentrations decreased  
38 from 2000 to 2019, but annual mean PM<sub>2.5</sub> concentrations still exceeded 35 μg m<sup>-3</sup> at  
39 74% of 1498 monitoring sites in 2015-2019. The concentration of PM<sub>2.5</sub> and its  
40 components were significantly higher (16%-195%) on hazy days than on non-hazy days.  
41 Compared with mean values of other components, this difference was more significant  
42 for the secondary inorganic ions SO<sub>4</sub><sup>2-</sup>, NO<sub>3</sub><sup>-</sup>, and NH<sub>4</sub><sup>+</sup> (average increase 98%). While  
43 sulfate concentrations significantly decreased over the time period, no significant  
44 change was observed for nitrate and ammonium concentrations. Model simulations  
45 indicate that the effectiveness of a 50% NH<sub>3</sub> emission reduction for controlling SIA  
46 concentrations decreased from 2010 to 2017 in four megacity clusters of eastern China,  
47 simulated for the month of January under fixed meteorological conditions (2010).  
48 Although the effectiveness further declined in 2020 for simulations including the  
49 natural experiment of substantial reductions in acid gas emissions during the COVID-  
50 19 pandemic, the resulting reductions in SIA concentrations were on average 20.8%  
51 lower than that in 2017. In addition, the reduction of SIA concentrations in 2017 was  
52 greater for 50% acid gas reductions than for the 50% NH<sub>3</sub> emissions reduction. Our  
53 findings indicate that persistent secondary inorganic aerosol pollution in China is  
54 limited by acid gases emissions, while an additional control on NH<sub>3</sub> emissions would  
55 become more important as reductions of SO<sub>2</sub> and NO<sub>x</sub> emissions progress.

56

57 **Keywords:** Air pollution, Particulate matter, Second inorganic aerosols, Anthropogenic  
58 emission, Ammonia.

59

## 60 **1. Introduction**

61 Over the past two decades, China has experienced severe PM<sub>2.5</sub> (particulate matter  
62 with aerodynamic diameter  $\leq 2.5 \mu\text{m}$ ) pollution (Huang et al., 2014; Wang et al., 2016),  
63 leading to adverse impacts on human health (Liang et al., 2020) and the environment  
64 (Yue et al., 2020). In 2019, elevated PM<sub>2.5</sub> concentrations accounted for 46% of polluted  
65 days in China and PM<sub>2.5</sub> was officially identified as a key year-round air pollutant  
66 (MEEP, 2019). Mitigation of PM<sub>2.5</sub> pollution is therefore the most pressing current  
67 challenge to improve China's air quality.

68 The Chinese government has put a major focus on particulate air pollution control  
69 through a series of policies, regulations, and laws to prevent and control severe air  
70 pollution. Before 2010, the Chinese government mainly focused on controlling SO<sub>2</sub>  
71 emissions via improvement of energy efficiency, with less attention paid to NO<sub>x</sub>  
72 abatement (CSC, 2007, 2011, 2016). For example, the 11<sup>th</sup> Five-Year Plan (FYP) (2006-  
73 2010) set a binding goal of a 10% reduction for SO<sub>2</sub> emission (CSC, 2007). The 12<sup>th</sup>  
74 FYP (2011-2015) added NO<sub>x</sub> regulation and required 8% and 10% reductions for SO<sub>2</sub>  
75 and NO<sub>x</sub> emissions, respectively (CSC, 2011) This was followed by further reductions  
76 in SO<sub>2</sub> and NO<sub>x</sub> emissions of 15% and 10%, respectively, in the 13<sup>th</sup> FYP (2016-2020)  
77 (CSC, 2016). In response to the severe haze events of 2013, the Chinese State Council  
78 promulgated the toughest-ever 'Atmospheric Pollution Prevention and Control Action  
79 Plan' in September 2013, aiming to reduce ambient PM<sub>2.5</sub> concentrations by 15-20% in  
80 2017 relative to 2013 levels in metropolitan regions (CSC, 2013). As a result of the  
81 implementation of stringent control measures, emissions reductions markedly

82 accelerated from 2013-2017, with decreases of 59% for SO<sub>2</sub>, 21% for NO<sub>x</sub>, and 33%  
83 for primary PM<sub>2.5</sub> (Zheng et al., 2018). Consequently, significant reductions in annual  
84 mean PM<sub>2.5</sub> concentrations were observed nationwide (Zhang et al., 2019; Yue et al.,  
85 2020), in the range 28-40% in the metropolitan regions (CSC, 2018a). To continue its  
86 efforts in tackling air pollution, China promulgated the Three-Year Action Plan (TYAP)  
87 in 2018 for Winning the Blue-Sky Defense Battle (CSC, 2018b), which required a  
88 further 15% reduction in NO<sub>x</sub> emissions by 2020 compared to 2018 levels.

89 Despite a substantial reduction in PM<sub>2.5</sub> concentrations in China, the proportion of  
90 secondary aerosols during severe haze periods is increasing (An et al., 2019), and can  
91 comprise up to 70% of PM<sub>2.5</sub> concentrations (Huang et al., 2014). Secondary inorganic  
92 aerosols (SIA, the sum of sulfate (SO<sub>4</sub><sup>2-</sup>), nitrate (NO<sub>3</sub><sup>-</sup>), and ammonium (NH<sub>4</sub><sup>+</sup>)) were  
93 found to be of equal importance to secondary organic aerosols, with 40-50%  
94 contributions to PM<sub>2.5</sub> in eastern China (Huang et al., 2014; Yang et al., 2011). The acid  
95 gases (i.e., NO<sub>x</sub>, SO<sub>2</sub>), together with NH<sub>3</sub>, are crucial precursors of SIA via chemical  
96 reactions that form particulate ammonium sulfate, ammonium bisulfate, and  
97 ammonium nitrate (Ianniello et al., 2010). In addition to the adverse impacts on human  
98 health via fine particulate matter formation (Liang et al., 2020; Kuerban et al., 2020),  
99 large amounts of NH<sub>3</sub> and its aerosol-phase products also lead to nitrogen deposition  
100 and consequently to environmental degradation (Ortiz-Montalvo et al., 2014; Pan et al.,  
101 2015; Xu et al., 2015, 2018; Zhan et al., 2021).

102 Following the successful controls on NO<sub>x</sub> and SO<sub>2</sub> emissions since 2013 in China,  
103 some studies found SO<sub>4</sub><sup>2-</sup> exhibited much larger decline than NO<sub>3</sub><sup>-</sup> and NH<sub>4</sub><sup>+</sup>, which  
104 lead to a rapid transition from sulfate-driven to nitrate-driven aerosol pollution (Li et  
105 al., 2019, 2021; Zhang et al., 2019). Attention is turning to NH<sub>3</sub> emissions as a possible  
106 means of further PM<sub>2.5</sub> control (Bai et al., 2019; Kang et al., 2016), particularly as

107 emissions of NH<sub>3</sub> increased between the 1980s and 2010s. Some studies have found  
108 that NH<sub>3</sub> limited the formation of SIA in winter in the eastern United States (Pinder et  
109 al., 2007) and Europe (Megaritis et al., 2013). Controls on NH<sub>3</sub> emissions have been  
110 proposed in the TYAP, although mandatory measures and binding targets have not yet  
111 been set (CSC, 2018b). Nevertheless, this proposal means that China will enter a new  
112 phase of PM<sub>2.5</sub> mitigation, with attention now given to both acid gas and NH<sub>3</sub> emissions.  
113 However, in the context of effective control of PM<sub>2.5</sub> pollution via its SIA component,  
114 two key questions arise: 1) what are the responses of the constituents of SIA to  
115 implementation of air pollution control policies, and 2) what is the relative efficiency  
116 of NH<sub>3</sub> versus acid gas emission controls to reduce SIA pollution?

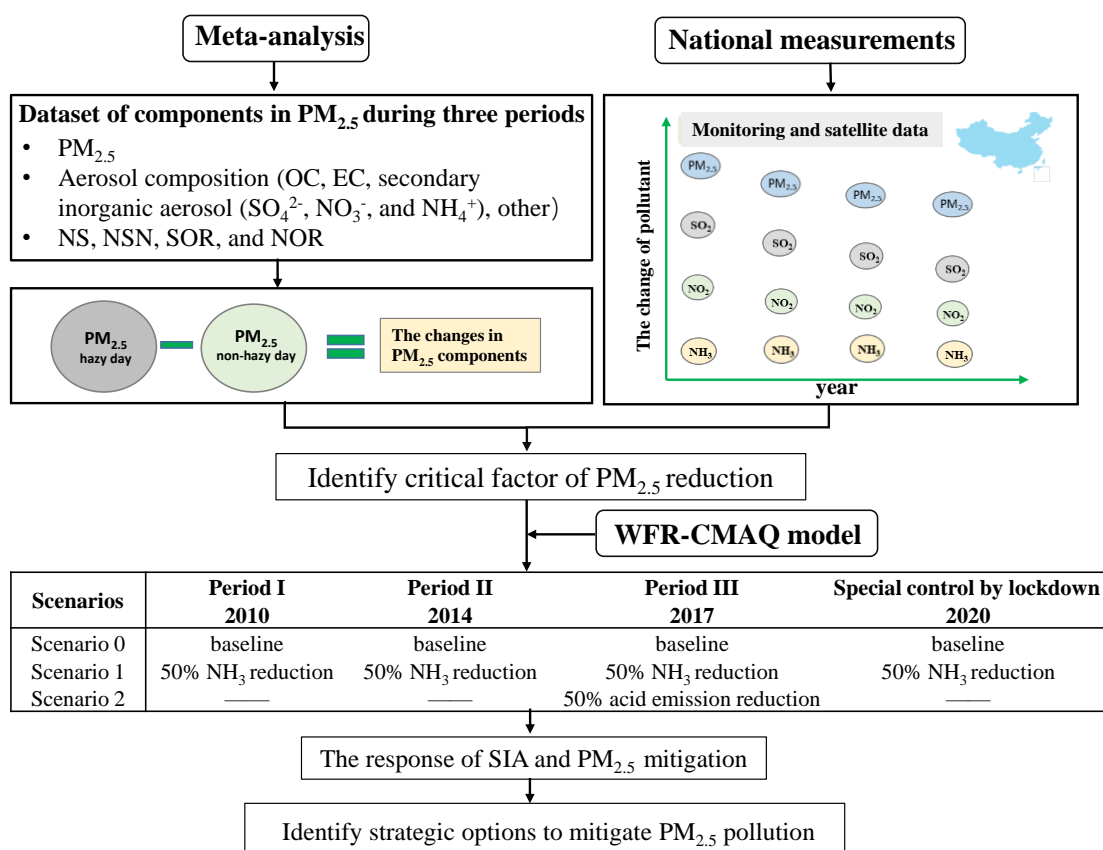
117 To fill this evidence gap and provide useful insights for policy-making to improve  
118 air quality in China, this study adopts an integrated assessment framework. With respect  
119 to the emission control policy summarized above, China's PM<sub>2.5</sub> control can be divided  
120 into three periods: period I (2000–2012), in which PM<sub>2.5</sub> was not the targeted pollutant;  
121 period II (2013–2016), the early stage of targeted PM<sub>2.5</sub> control policy implementation;  
122 and period III (2017–2019), the latter stage with more stringent policies. Therefore, our  
123 research framework consists of two parts: (1) assessment of trends in annual mean  
124 concentrations of PM<sub>2.5</sub>, its chemical components and SIA gaseous precursors from  
125 meta-analyses and observations; (2) quantification of SIA responses to emissions  
126 reductions in NH<sub>3</sub> and acid gases using the Weather Research and Forecasting and  
127 Community Multiscale Air Quality (WRF/CMAQ) models.

## 128 **2. Materials and methods**

### 129 **2.1. Research framework**

130 This study developed an integrated assessment framework to analysis the trends of  
131 secondary inorganic aerosol and strategic options to reduce SIA and PM<sub>2.5</sub> pollution in

132 China (Fig. 1). The difference in PM<sub>2.5</sub> chemical components between hazy and non-  
 133 hazy days was first assessed by meta-analysis of published studies. These were  
 134 interpreted in conjunction with the trends in air concentrations of PM<sub>2.5</sub> and its  
 135 secondary inorganic aerosol precursors (SO<sub>2</sub>, NO<sub>2</sub>, and NH<sub>3</sub>) derived from surface  
 136 measurements and satellite observations. The potential of SIA and PM<sub>2.5</sub> concentration  
 137 reductions from precursor emission reductions was then evaluated using the Weather  
 138 Research and Forecasting and Community Multiscale Air Quality (WRF/CMAQ)  
 139 models.



140

141 **Fig. 1.** Integrated assessment framework for Chinese PM<sub>2.5</sub> mitigation strategic options.

142 OC is organic carbon, EC is elemental carbon, NO<sub>3</sub><sup>-</sup> is nitrate, SO<sub>4</sub><sup>2-</sup> is sulfate, and NH<sub>4</sub><sup>+</sup>

143 is ammonium. NS is the slope of the regression equation between [NH<sub>4</sub><sup>+</sup>] and [SO<sub>4</sub><sup>2-</sup>],

144 NSN is the slope of the regression equation between [NH<sub>4</sub><sup>+</sup>] and [SO<sub>4</sub><sup>2-</sup> + NO<sub>3</sub><sup>-</sup>], SOR

145 is sulfur oxidation ratio, and NOR is nitrogen oxidation ratio. SIA is secondary

146 inorganic aerosols. WRF-CMAQ is Weather Research and Forecasting and Community  
147 Multiscale Air Quality models.

## 148 **2.2. Meta-analysis of PM<sub>2.5</sub> and its chemical components**

149 Meta-analyses can be used to quantify the differences in concentrations of PM<sub>2.5</sub> and  
150 its secondary inorganic aerosol components (NH<sub>4</sub><sup>+</sup>, NO<sub>3</sub><sup>-</sup>, and SO<sub>4</sub><sup>2-</sup>) between hazy and  
151 non-hazy days and to identify the major pollutants on non-hazy days (Wang et al.,  
152 2019b); this provides evidence for effective options on control of precursor emissions  
153 (NH<sub>3</sub>, NO<sub>2</sub>, and SO<sub>2</sub>) for reducing occurrences of hazy days. To build a database of  
154 atmospheric concentrations of PM<sub>2.5</sub> and chemical components between hazy and non-  
155 hazy days, we conducted a literature survey using the Web of Science and the China  
156 National Knowledge Infrastructure for papers published between January 2000 and  
157 January 2020. The keywords included: (1) "particulate matter," or "aerosol," or "PM<sub>2.5</sub>"  
158 and (2) "China" or "Chinese". Studies were selected based on the following conditions:  
159 (1) Measurements were taken on both hazy and non-hazy days.  
160 (2) PM<sub>2.5</sub> chemical components were reported.  
161 (3) If hazy days were not defined in the screened articles, the days with PM<sub>2.5</sub>  
162 concentrations > 75 µg m<sup>-3</sup> (the Chinese Ambient Air Quality Standard Grade II for  
163 PM<sub>2.5</sub> (CSC, 2012)) were treated as hazy days.  
164 (4) If an article reported measurements from different monitoring sites in the same city,  
165 e.g. Mao et al. (2018) and Xu et al. (2019), then each measurement was considered an  
166 independent study.  
167 (5) If there were measurements in the same city for the same year, e.g. Tao et al. (2016)  
168 and Han et al. (2017), then each measurement was treated as an independent study.

169 One hundred articles were selected based on the above conditions with the lists  
170 provided in the Supporting Material dataset. For each selected study, we documented

171 the study sites, study periods, seasons, aerosol types, and aerosol species mass  
172 concentrations (in  $\mu\text{g m}^{-3}$ ) over the entire study period (2000–2019) (the detailed data  
173 are provided in the dataset). In total, the number of sites contributing data to the meta-  
174 analysis was 267 and their locations are shown in [Fig. S1](#). If relevant data were not  
175 directly presented in studies, a GetData Graph Digitizer (Version 2.25,  
176 <http://www.getdatagraph-digitizer.com>) was used to digitize concentrations of  $\text{PM}_{2.5}$   
177 chemical components from figures. The derivations of other variables such as sulfur  
178 and nitrogen oxidation ratios are described in [Supplementary Information Method 1](#).

179 Effect sizes were developed to normalize the combined studies' outcomes to the  
180 same scale. This was done through the use of log response ratios (lnRR) ([Nakagawa et  
181 al., 2012; Ying et al., 2019](#)). The variations in aerosol species were evaluated as follows:

$$182 \ln RR = \ln \left( \frac{X_p}{X_n} \right) \quad (1)$$

183 where  $X_p$  and  $X_n$  represent the mean values of the studied variables of  $\text{PM}_{2.5}$  components  
184 on hazy and non-hazy days, respectively. The mean response ratio was then estimated  
185 as:

$$186 RR = \exp \left[ \frac{\sum \ln RR(i) \times W(i)}{\sum W(i)} \right] \quad (2)$$

187 where  $W(i)$  is the weight given to that observation as described below. Finally, variable-  
188 related effects were expressed as percent changes, calculated as  $(RR-1) \times 100\%$ . A 95%  
189 confidence interval not overlapping with zero indicates that the difference is significant.  
190 A positive or negative percentage value indicates an increase or decrease in the response  
191 variables, respectively.

192 We used inverse sampling variances to weight the observed effect size (RR) in the  
193 meta-analysis ([Benitez-Lopez et al., 2017](#)). For the measurement sites where standard  
194 deviations (SD) or standard errors (SE) were absent in the original study reports, we  
195 used the "Bracken, 1992" approach to estimate SD ([Bracken et al., 1992](#)). The variation-



196 related chemical composition of PM<sub>2.5</sub> was assessed by random effects in meta-analysis.  
197 Rosenberg's fail safe-numbers ( $N_{fs}$ ) were calculated to assess the robustness of findings  
198 on PM<sub>2.5</sub> to publication bias (Ying et al., 2019) (See Table S1). The results (effects)  
199 were considered robust despite the possibility of publication bias if  $N_{fs} > 5 \times n + 10$ ,  
200 where  $n$  indicates the number of sites. The statistical analysis of the concentrations of  
201 PM<sub>2.5</sub> and secondary inorganic ions for three periods used a non-parametric statistical  
202 method since concentrations were not normally distributed based on the Kruskal-Wallis  
203 test (Kruskal and Walls, 1952). For each species, the Kruskal-Wallis one-way analysis  
204 of variance (ANOVA) on ranks among three periods was performed with pairwise  
205 comparison using Dunn's method (Dunn, 1964).

### 206 **2.3. Data collection of air pollutant concentrations**

207 To assess the recent annual trends in China of PM<sub>2.5</sub> and of the SO<sub>2</sub> and NO<sub>2</sub>  
208 gaseous precursors to SIA, real-time monitoring data of these pollutants at 1498  
209 monitoring stations in 367 cities during 2015–2019 were obtained from the China  
210 National Environmental Monitoring Center (CNEMC) (<http://106.37.208.233:20035/>).  
211 This is an open-access archive of air pollutant measurements from all prefecture-level  
212 cities since January 2015. Successful use of data from CNEMC to determine  
213 characteristics of air pollution and related health risks in China has been demonstrated  
214 previously (Liu et al., 2016; Kuerban et al., 2020). The geography stations are shown  
215 in Fig. S1. The annual mean concentrations of the three pollutants at all sites were  
216 calculated from the hourly time-series data according to the method of Kuerban et al.  
217 (2020). Information about sampling instruments, sampling methods, and data quality  
218 controls for PM<sub>2.5</sub>, SO<sub>2</sub>, and NO<sub>2</sub> is provided in Supplementary Method 2. Surface NH<sub>3</sub>  
219 concentrations over China for the 2008–2016 (the currently available) were extracted  
220 from the study of Liu et al. (2019a). Further details are in Supplementary Method 2.

## 221 **2.4. WRF/CMAQ model simulations**

222 The Weather Research and Forecasting model (WRFv3.8) and the Models-3  
223 community multi-scale air quality (CMAQv5.2) model were used to evaluate the  
224 impacts of emission reductions on SIA and PM<sub>2.5</sub> concentrations over China. The  
225 simulations were conducted at a horizontal resolution of 12 km × 12 km. The simulation  
226 domain covered the whole of China, part of India and east Asia. In the current study,  
227 focus was on the following four regions in China: Beijing-Tianjin-Hebei (BTH),  
228 Yangtze River Delta (YRD), Pearl River Delta (PRD), and Sichuan Basin (SCB). The  
229 model configurations used in this study were the same as those used in [Wu et al. \(2018a\)](#)  
230 and are briefly described here. The WRFv3.8 model was applied to generate  
231 meteorological inputs for the CMAQ model using the National Center for  
232 Environmental Prediction Final Operational Global Analysis (NCEP-FNL) dataset  
233 ([Morrison et al., 2009](#)). Default initial and boundary conditions were used in the  
234 simulations. The carbon-bond (CB05) gas-phase chemical mechanism and AERO6  
235 aerosol module were selected in the CMAQ configuration ([Guenther et al., 2012](#)).  
236 Anthropogenic emissions for 2010, 2014 and 2017 were obtained from the Multi-  
237 resolution Emission Inventory (<http://meicmodel.org>) with 0.25° × 0.25° spatial  
238 resolution and aggregated to 12 km×12 km resolution ([Zheng et al., 2018](#); [Li et al.,](#)  
239 [2017](#)). Each simulation was spun-up for six days in advance to eliminate the effects of  
240 the initial conditions.

241 The years 2010, 2014 and 2017 were chosen to represent the anthropogenic  
242 emissions associated with the periods I, II, III, respectively. January was selected as the  
243 typical simulation month because wintertime haze pollution frequently occurs in this  
244 month ([Wang et al., 2011](#); [Liu et al., 2019b](#)). January of 2010 was also found to have  
245 PM<sub>2.5</sub> pollution more serious than other months ([Geng et al., 2017, 2021](#)). The

246 sensitivity scenarios of emissions in January can therefore help to identify the efficient  
247 option to control haze pollution.

248 The Chinese government has put a major focus on acid gas emission control  
249 through a series of policies in the past three periods (Fig. S2). The ratio decreases of  
250 anthropogenic emissions SO<sub>2</sub> and NO<sub>x</sub> in January for the years 2010, 2014, 2017 and  
251 2020 are presented in SI Tables S2 and S3, respectively. The emissions from  
252 surrounding countries were obtained from the Emissions Database for Global  
253 Atmospheric Research (EDGAR): HTAPV2. The scenarios and the associated  
254 reductions of NH<sub>3</sub>, NO<sub>x</sub> and SO<sub>2</sub> for selected four years in three periods can be found  
255 in Fig. 1.

256 The sensitivities of SIA and PM<sub>2.5</sub> to NH<sub>3</sub> emissions reductions were determined  
257 from the average PM<sub>2.5</sub> concentrations in model simulations without and with an  
258 additional 50% NH<sub>3</sub> emissions reduction. The choice of 50% additional NH<sub>3</sub> emissions  
259 reduction is based on the feasibility and current upper bound of NH<sub>3</sub> emissions  
260 reduction expected to be realized in the near future (Liu et al., 2019a; Zhang et al.,  
261 2020a; Table S4). For example, Zhang et al. (2020a) found that the mitigation potential  
262 of NH<sub>3</sub> emissions from cropland production and livestock production in China can  
263 reach up to 52% and 58%, respectively. To eliminate the influences of varying  
264 meteorological conditions, all simulations were conducted under the fixed  
265 meteorological conditions of 2010.

266 During the COVID-19 lockdown in China, emissions of primary pollutants were  
267 subject to unprecedented reductions due to national restrictions on traffic and industry;  
268 in particular, emissions of NO<sub>x</sub> and SO<sub>2</sub> reduced by 46% and 24%, respectively,  
269 averaged across all Chinese provinces (Huang et al., 2021). We therefore also ran  
270 simulations applying the same reductions in NO<sub>x</sub> and SO<sub>2</sub> (based on 2017 MEIC) that

271 were actually observed during the COVID-19 lockdown as a case of special control in  
272 2020.

## 273 **2.5 Model performance**

274 The CMAQ model has been extensively used in air quality studies (Zhang et al.,  
275 2019; Backes et al., 2016) and the validity of the chemical regime in the CMAQ model  
276 had been confirmed by our previous studies (Zhang et al., 2021a; Wang et al., 2020a,  
277 2021a). In this study, we used surface measurements from previous publications (e.g.,  
278 (Xiao et al., 2020, 2021; Geng et al., 2019; Xue et al., 2019) and satellite observations  
279 to validate the modelling meteorological parameters by WRF model and air  
280 concentrations of PM<sub>2.5</sub> and associated chemical components by CMAQ model. The  
281 meteorological measurements used for validating the WRF model performances were  
282 obtained from the National Climate Data Center (NCDC)  
283 (<ftp://ftp.ncdc.noaa.gov/pub/data/noaa/>). For validation of the CMAQ model, monthly  
284 mean concentrations of PM<sub>2.5</sub> were obtained from ChinaHighAirPollutants (CHAP,  
285 <https://weijing-rs.github.io/product.html>) database. We also collected ground-based  
286 observations from previous publications to validate the modeling concentrations of  
287 SO<sub>4</sub><sup>2-</sup>, NO<sub>3</sub><sup>-</sup>, and NH<sub>4</sub><sup>+</sup>. The detailed information of the monitoring sites is presented in  
288 Table S5. Further information about the modelling is given in Supplementary Method  
289 3 and Figs. S3-S7 and Table S5.

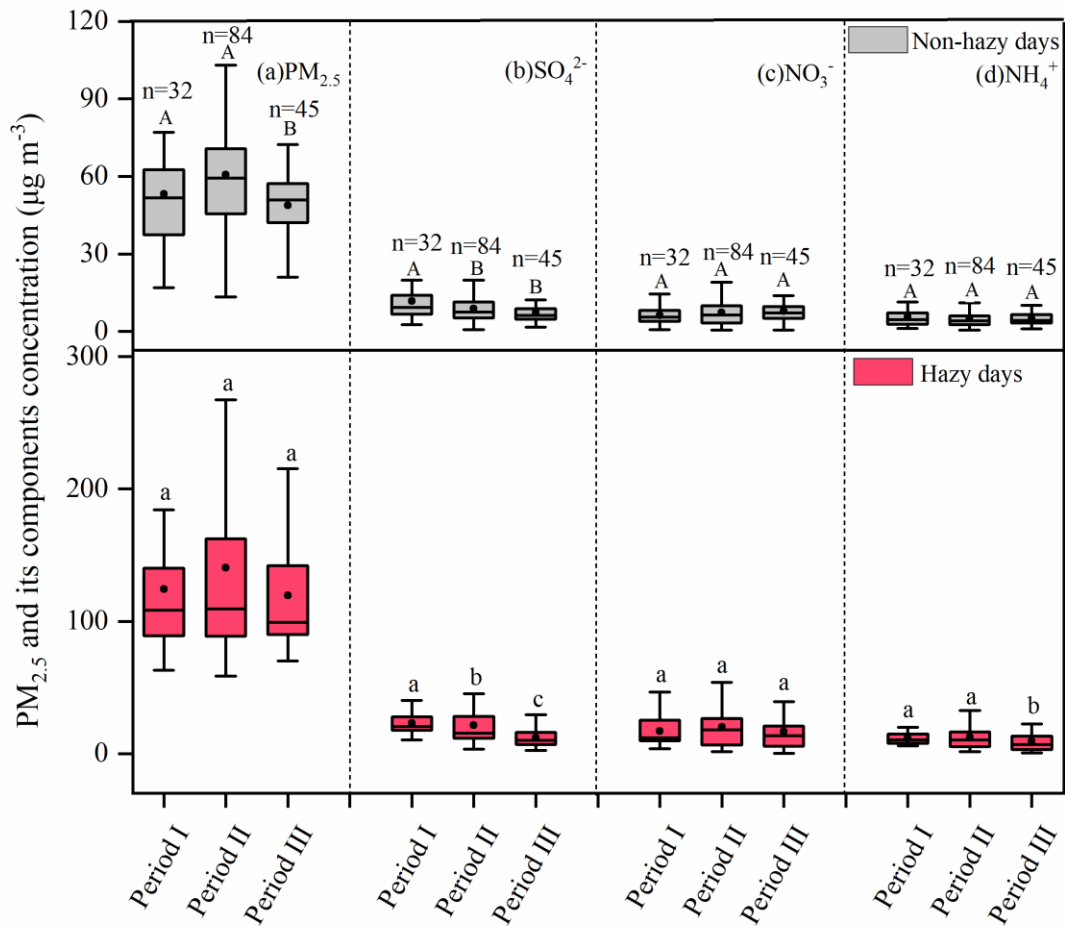
## 290 **3. Results and discussion**

### 291 **3.1. Characteristics of PM<sub>2.5</sub> and its chemical components from the meta-analysis** 292 **and from nationwide observations**

293 The meta-analysis based on all published analyses of PM<sub>2.5</sub> and chemical  
294 component measurements during 2000–2019 reveals the changing characteristics of  
295 PM<sub>2.5</sub>. To assess the annual trends in PM<sub>2.5</sub> and its major chemical components, we

296 made a three-period comparison using the measurements at sites that include both PM<sub>2.5</sub>  
297 and secondary inorganic ions SO<sub>4</sub><sup>2-</sup>, NO<sub>3</sub><sup>-</sup>, and NH<sub>4</sub><sup>+</sup> (Fig. 2). The PM<sub>2.5</sub> concentrations  
298 on both hazy and non-hazy days showed no significant trend from period I to period II  
299 based on the Kruskal-Wallis test. This could be explained by the enhanced atmospheric  
300 oxidation capacity (Huang et al., 2021), faster deposition of total inorganic nitrate (Zhai  
301 et al., 2021) and the changes of atmospheric circulation (Zheng et al., 2015; Li et al.,  
302 2020). However, the observed concentrations of PM<sub>2.5</sub> showed a downward trend from  
303 Period I to Period III on the non-hazy days, decreasing by 8.2% (Fig. 2a), despite no  
304 significant decreasing trend on the hazy days (Fig. 2a). In addition, the annual mean  
305 PM<sub>2.5</sub> concentrations from the nationwide measurements showed declining trends  
306 during 2015-2019 averaged across all China and for each of the BTH, YRD, SCB, and  
307 PRD megacity clusters of eastern China (Fig. 3a, d).

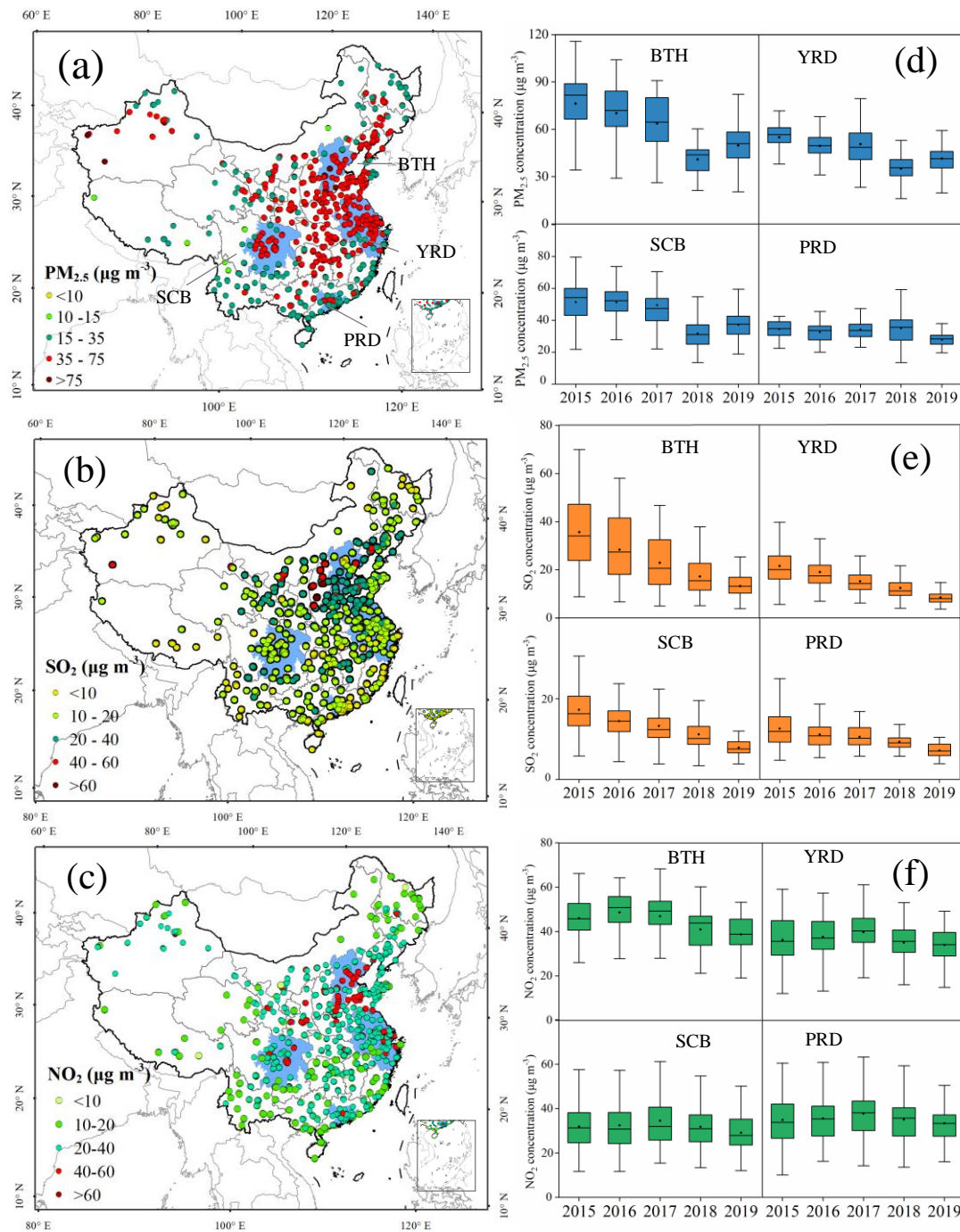
308 These results reflect the effectiveness of the pollution control policies (Fig. S2)  
309 implemented by the Chinese government at the national scale. Nevertheless, PM<sub>2.5</sub>  
310 remained at relatively high levels. Over 2015–2019, the annual mean PM<sub>2.5</sub>  
311 concentrations at 74% of the 1498 sites (averaging  $51.9 \pm 12.4 \mu\text{g m}^{-3}$ , Fig. 3a) exceeded  
312 the Chinese Grade-II Standard (GB 3095–2012) of  $35 \mu\text{g m}^{-3}$  (MEPC, 2012), indicating  
313 that PM<sub>2.5</sub> mitigation is a significant challenge for China.



314

315 **Fig. 2.** Comparisons of observed concentrations of (a) PM<sub>2.5</sub>, (b) SO<sub>4</sub><sup>2-</sup>, (c) NO<sub>3</sub><sup>-</sup>, and  
 316 (d) NH<sub>4</sub><sup>+</sup> between non-hazy and hazy days in Period I (2000–2012), Period II (2013–  
 317 2016), and Period III (2017–2019). Bars with different letters denote significant  
 318 differences among the three periods ( $P < 0.05$ ) (upper and lowercase letters for non-  
 319 hazy and hazy days, respectively). The upper and lower boundaries of the boxes  
 320 represent the 75th and 25th percentiles; the line within the box represents the median  
 321 value; the whiskers above and below the boxes represent the 90th and 10th percentiles;  
 322 the point within the box represents the mean value. Comparison of the pollutants among  
 323 the three-periods using Kruskal-Wallis and Dunn's test. The  $n$  represents independent  
 324 sites; more detail on this is presented in [Section 2.2](#).

325



326

327 **Fig. 3.** Left: spatial patterns of annual mean observed concentration of (a) PM<sub>2.5</sub>, (b)  
 328 SO<sub>2</sub>, (c) NO<sub>2</sub> at 1498 sites, averaged for 2015–2019. Right: the annual observed  
 329 concentrations of (d) PM<sub>2.5</sub>, (e) SO<sub>2</sub>, and (f) NO<sub>2</sub> for 2015-2019 in four megacity  
 330 clusters (BTH: Beijing-Tianjin-Hebei, YRD: Yangtze River Delta, SCB: Sichuan Basin,  
 331 PRD: Pearl River Delta). The locations of the regions are indicated by the blue shading  
 332 on the map. The upper and lower boundaries of the boxes represent the 75th and 25th

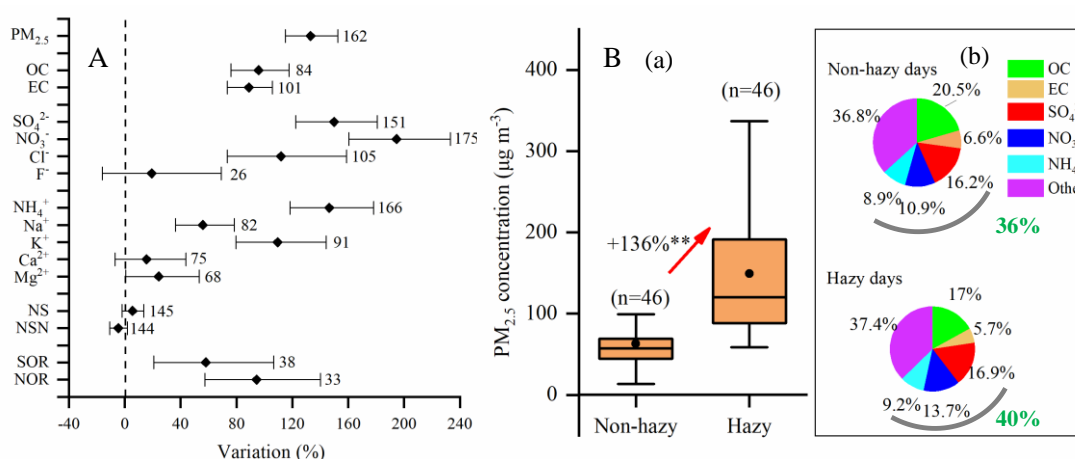
333 percentiles; the line within the box represents the median value; the whiskers above and  
334 below the boxes represent the 90th and 10th percentiles; the point within the box  
335 represents the mean value.

336 To further explore the underlying drivers of PM<sub>2.5</sub> pollution, we analyzed the  
337 characteristics of PM<sub>2.5</sub> chemical components and their temporal changes in China. The  
338 concentrations of PM<sub>2.5</sub> and all its chemical components (except F<sup>-</sup> and Ca<sup>2+</sup>) were  
339 significantly higher on hazy days than on non-hazy days (Fig. 4A). Compared with  
340 other components this difference was more significant for secondary inorganic ions (i.e.,  
341 SO<sub>4</sub><sup>2-</sup>, NO<sub>3</sub><sup>-</sup>, and NH<sub>4</sub><sup>+</sup>). Sulfur oxidation ratio (SOR) and nitrogen oxidation ratio  
342 (NOR) were also 58.0% and 94.4% higher on hazy days than on non-hazy days,  
343 respectively, implying higher oxidations of gaseous species to sulfate- and nitrate-  
344 containing aerosols on the hazy days (Sun et al., 2006; Xu et al., 2017).

345 To provide quantitative information on differences in PM<sub>2.5</sub> and its components  
346 between hazy days and non-hazy days, we made a comparison using 46 groups of data  
347 on simultaneous measurements of PM<sub>2.5</sub> and chemical components. The 46 groups refer  
348 to independent analyses from the literature that compare concentrations of PM<sub>2.5</sub> and  
349 major components (SO<sub>4</sub><sup>2-</sup>, NO<sub>3</sub><sup>-</sup>, NH<sub>4</sub><sup>+</sup>, OC, and EC) on hazy and non-hazy days  
350 measured across different sets of sites. The “Other” species was calculated by  
351 difference between PM<sub>2.5</sub> and sum of OC, EC, and secondary inorganic ions (SO<sub>4</sub><sup>2-</sup>,  
352 NO<sub>3</sub><sup>-</sup> and NH<sub>4</sub><sup>+</sup>). As shown in Fig.4B (a), PM<sub>2.5</sub> concentrations significantly increased  
353 (by 136%) on the hazy days (149.2 ± 81.6 μg m<sup>-3</sup>) relative to those on the non-hazy  
354 days (63.2 ± 29.8 μg m<sup>-3</sup>). By contrast, each component’s proportions within PM<sub>2.5</sub>  
355 differed slightly, with 36% and 40% contributions by SIA on non-hazy days and hazy  
356 days, respectively (Fig. 4B(b)). This is not surprising because concentrations of PM<sub>2.5</sub>  
357 and SIA both significantly increased on the hazy days (60.1 ± 37.4 μg m<sup>-3</sup> for SIA)



358 relative to the non-hazy days ( $22.4 \pm 12.1 \mu\text{g m}^{-3}$  for SIA). Previous studies have found  
 359 that increased SIA formation is the major influencing factor for haze pollution in  
 360 wintertime and summertime (mainly in years since 2013) in major Chinese cities in  
 361 eastern China (Huang et al., 2014; Wang et al., 2019a; Li et al., 2018). Our results  
 362 extend confirmation of the dominant role of SIA to PM<sub>2.5</sub> pollution over a large spatial  
 363 scale in China and to longer temporal scales.



364 **Fig. 4.** (A) Variations in PM<sub>2.5</sub> concentration, aerosol component concentration, NS,  
 365 NSN, SOR, and NOR from non-hazy to hazy days in China during 2000–2019. (B) (a)  
 366 Summary of differences in PM<sub>2.5</sub> concentration between non-hazy and hazy days in  
 367 China; (b) the average proportions of components of PM<sub>2.5</sub> on non-hazy and hazy days.  
 368 NS is the slope of the regression equation between [NH<sub>4</sub><sup>+</sup>] and [SO<sub>4</sub><sup>2-</sup>], NSN is the slope  
 369 of the regression equation between [NH<sub>4</sub><sup>+</sup>] and [SO<sub>4</sub><sup>2-</sup> + NO<sub>3</sub><sup>-</sup>], SOR is sulfur oxidation  
 370 ratio, and NOR is nitrogen oxidation ratio. The variations are considered significant if  
 371 the confidence intervals of the effect size do not overlap with zero. \*\* denotes significant  
 372 difference ( $P < 0.01$ ) between hazy days and non-hazy days. The upper and lower  
 373 boundaries of the boxes represent the 75th and 25th percentiles; the line within the box  
 374 represents the median value; the whiskers above and below the boxes represent the 90th  
 375 and 10th percentiles; the point within the box represents the mean value. Values  
 376 adjacent to each confidence interval indicate number of measurement sites. The  $n$   
 377

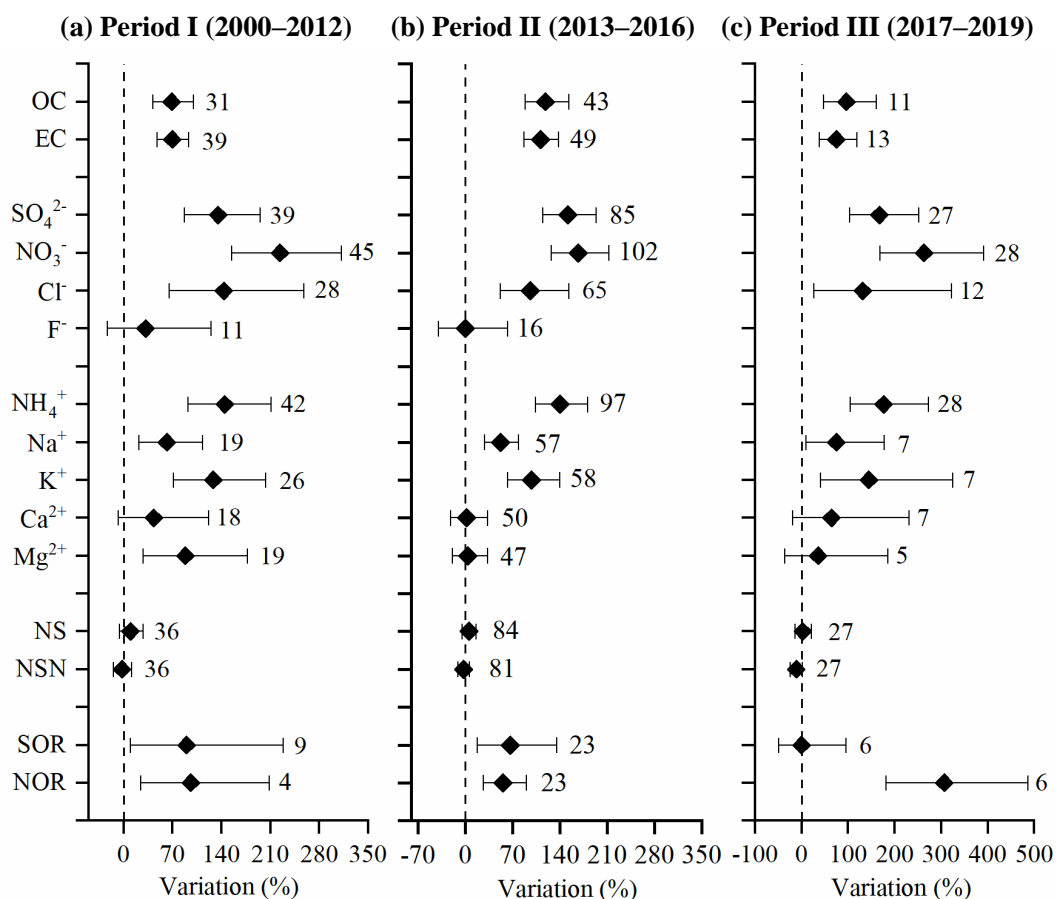
378 represents independent sites; more detail on this is presented in [Section 2.2](#).

379 The effect values of SIA on the hazy days were significantly higher than those on  
380 non-hazy days for all three periods (I, II, and III) ([Fig. 5](#)), indicating the persistent  
381 prevalence of the SIA pollution problem over the past two decades. Considering  
382 changes in concentrations,  $\text{SO}_4^{2-}$  showed a downward trend from Period I to Period III  
383 on the non-hazy days and hazy day, decreasing by 38.6% and 48.3%, respectively ([Fig.](#)  
384 [2b](#)). These results reflect the effectiveness of the  $\text{SO}_2$  pollution control policies ([Ronald](#)  
385 [et al., 2017](#)). In contrast, there were no significant downward trends in concentrations  
386 of  $\text{NO}_3^-$  and  $\text{NH}_4^+$  on either hazy or non-hazy days ([Fig. 2c, d](#)), but the mean  $\text{NO}_3^-$   
387 concentration in Period III decreased by 10.5% compared with that in Period II,  
388 especially on hazy days (-16.8%). These results could be partly supported by decreased  
389  $\text{NO}_x$  emissions and tropospheric  $\text{NO}_2$  vertical column densities between 2011 and 2019  
390 in China owing to effective  $\text{NO}_x$  control policies ([Zheng et al., 2018](#); [Fan et al., 2021](#)).  
391 The lack of significantly downward trends in  $\text{NH}_4^+$  concentrations is due to the fact that  
392 the total  $\text{NH}_3$  emissions in China changed little and remained at high levels between  
393 2000 and 2018, i.e., slightly decreased from 2000 (10.3 Tg) to 2012 (9.3 Tg) ([Kang et](#)  
394 [al., 2016](#)) and then slightly increased between 2013 and 2018 ([Liu et al., 2021](#)). The  
395 same trends are also found in Quzhou in China, which is a long-term in situ monitoring  
396 site (in Quzhou County, North China Plain, operated by our group; the detailed  
397 information on Quzhou can be found in [Meng et al. \(2022\)](#) and [Feng et al. \(2022\)](#))  
398 during the period 2012-2020 from previous publications ([Xu et al., 2016](#); [Zhang et al.,](#)  
399 [2021b](#), noted that data during 2017-2020 are unpublished before) ([Fig. S8](#)). [Zhang et](#)  
400 [al. \(2020b\)](#) found that the clean air actions implemented in 2017 effectively reduced  
401 wintertime concentrations of  $\text{PM}_{10}$  (particulate matter with diameter  $\leq 10 \mu\text{m}$ ),  $\text{SO}_4^{2-}$  and

402  $\text{NH}_4^+$  in Beijing compared with those in 2007, but had no apparent effect on  $\text{NO}_3^-$ . Li  
403 et al. (2021) also found that  $\text{SO}_4^{2-}$  exhibited a significant decline, However,  $\text{NO}_3^-$  did  
404 not evidently exhibit a decreasing trend in the BTH region.

405 Our findings are to some extent supported by the nationwide measurements.  
406 Annual mean  $\text{SO}_2$  concentrations displayed a clear decreasing trend with a 53%  
407 reduction in 2019 relative to 2015 for the four megacity clusters of eastern China (Fig.  
408 3b, e), whereas there were only slight reductions in annual mean  $\text{NO}_2$  concentrations  
409 (Fig. 3c, f). In contrast, annual mean  $\text{NH}_3$  concentrations showed an obvious increasing  
410 trend in in both northern and southern regions of China, and especially in the BTH  
411 region (Fig. S9).

412 Overall, the above analyses indicate that  $\text{SO}_4^{2-}$  concentrations responded  
413 positively to air policy implementations at the national scale, but that reducing  $\text{NO}_3^-$   
414 and  $\text{NH}_4^+$  remains a significant challenge. China has a history of around 10-20 years  
415 for  $\text{SO}_2$  and  $\text{NO}_x$  emission control and has advocated  $\text{NH}_3$  controls despite to date no  
416 mandatory measures and binding targets having been set (Fig. S2). Nevertheless,  $\text{PM}_{2.5}$   
417 pollution, especially SIA such as  $\text{NO}_3^-$  and  $\text{NH}_4^+$ , is currently a serious problem (Fig. 4  
418 and 5a, b). Some studies have reported that  $\text{PM}_{2.5}$  pollution can be effectively reduced  
419 if implementing synchronous  $\text{NH}_3$  and  $\text{NO}_x/\text{SO}_2$  controls (Liu et al., 2019b). Therefore,  
420 based on the above findings, we propose that  $\text{NH}_3$  and  $\text{NO}_x/\text{SO}_2$  emission mitigation  
421 should be simultaneously strengthened to mitigate haze pollution.



422

423 **Fig. 5.** Variations in PM<sub>2.5</sub> composition, NS, NSN, SOR, and NOR from non-hazy to  
 424 hazy days in (a) Period I (2000–2012), (b) Period II (2013–2016), (c) Period III (2017–  
 425 2019). NS is the slope of the regression equation between [NH<sub>4</sub><sup>+</sup>] and [SO<sub>4</sub><sup>2-</sup>], NSN is  
 426 the slope of the regression equation between [NH<sub>4</sub><sup>+</sup>] and [SO<sub>4</sub><sup>2-</sup> + NO<sub>3</sub><sup>-</sup>], SOR is sulfur  
 427 oxidation ratio, and NOR is nitrogen oxidation ratio. The variations are statistically  
 428 significant if the confidence intervals of the effect size do not overlap with zero. Values  
 429 adjacent to each confidence interval indicate number of measurement sites. The *n*  
 430 represents independent sites; more detail on this is presented in [Section 2.2](#).

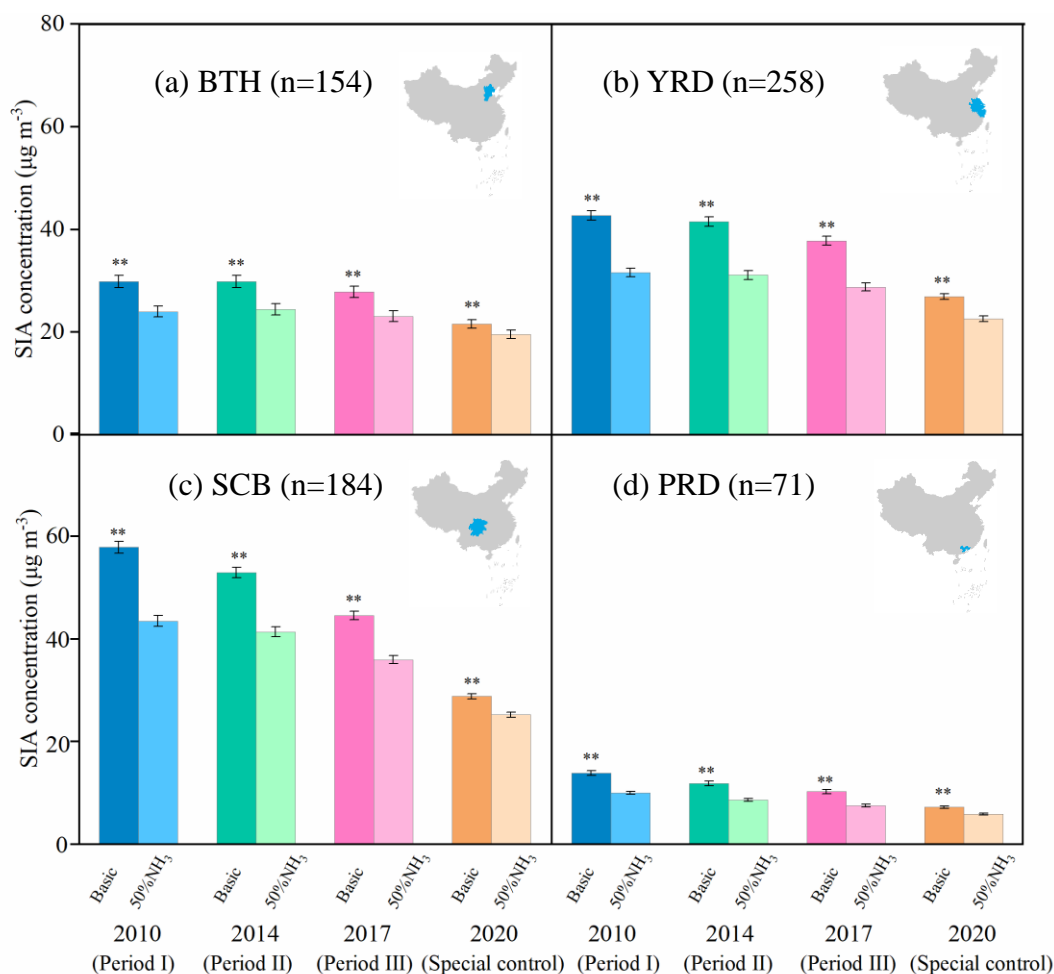
### 431 3.2. Sensitivities from model simulations

432 To further examine the efficiencies of NH<sub>3</sub> and acid gas emission reductions on  
 433 SIA and PM<sub>2.5</sub> mitigation, the decreases of mean SIA and PM<sub>2.5</sub> concentrations with and  
 434 without additional 50% NH<sub>3</sub> reductions were simulated using the WRF/CMAQ model.

435 Fig. 6 and Fig. S10 shows that, compared to 2010, SIA and PM<sub>2.5</sub> concentrations in  
436 January in 2017 were significantly decrease in the BTH, YRD, SCB, and PRD megacity  
437 clusters, respectively, in the simulations without additional NH<sub>3</sub> emission reductions.  
438 Across the four megacity clusters, the reduction in SIA and PM<sub>2.5</sub> is largest in the SCB  
439 region from 2010 to 2017 and smallest in the PRD region.

440 When simulating the effects of an additional 50% NH<sub>3</sub> emissions reductions in  
441 January in each of the years 2010, 2014 and 2017, the SIA concentrations in the  
442 megacity clusters (i.e. BTH, YRD, SCB and PRD) decreased by  $25.9 \pm 0.3\%$ ,  $24.4 \pm$   
443  $0.3\%$ , and  $22.9 \pm 0.3\%$ , respectively (Fig. 6 , Fig. S11, and Table S6). The reductions  
444 of PM<sub>2.5</sub> in 2010, 2014 and 2017 were  $9.7 \pm 0.1\%$ ,  $9.0 \pm 0.1\%$ , and  $9.2 \pm 0.2\%$  in  
445 the megacity clusters, respectively (Figs. S10 and S12). Whilst these results confirm  
446 the effectiveness of NH<sub>3</sub> emission controls, it is important to note that the response of  
447 SIA concentrations is less sensitive to additional NH<sub>3</sub> emission controls along the  
448 timeline of the SO<sub>2</sub> and NO<sub>x</sub> anthropogenic emissions reductions associated with the  
449 series of clean air actions implemented by the Chinese government from 2010 to 2017  
450 (Zheng et al., 2018). Given the feasibility and current upper bound of NH<sub>3</sub> emission  
451 reductions options in the near future (50%) (Liu et al., 2019b), further abatement of SIA  
452 concentrations merely by reducing NH<sub>3</sub> emissions is limited in China. In other words,  
453 the controls on acid gas emissions should continue to be strengthened beyond their  
454 current levels.

455

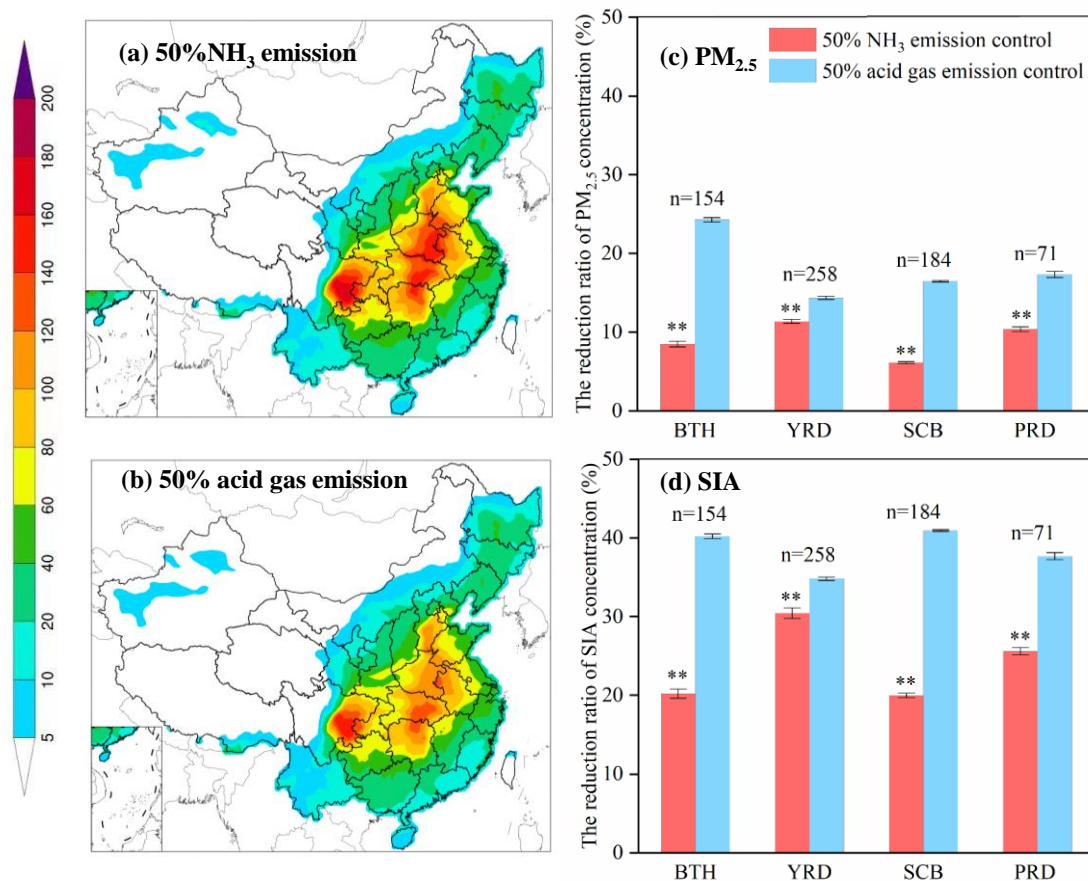


456

457 **Fig. 6.** Simulated SIA concentrations (in  $\mu\text{g m}^{-3}$ ) without (basic) and with 50%  
 458 ammonia ( $\text{NH}_3$ ) emissions reductions in January for the years 2010, 2014, 2017 and  
 459 2020 in four megacity clusters (BTH: Beijing-Tianjin-Hebei, YRD: Yangtze River  
 460 Delta, SCB: Sichuan Basin, PRD: Pearl River Delta). Inset maps indicate the location  
 461 of each region. \*\* denotes significant difference without and with 50% ammonia  
 462 emission reductions ( $P < 0.05$ ).  $n$  is the number of calculated samples by grid extraction.  
 463 Error bars are standard errors of means. (Period I (2000–2012), Period II (2013–2016),  
 464 and Period III (2017–2019); Special control is the restrictions in economic activities  
 465 and associated emissions during the COVID-19 lockdown period in 2020).

466 To further verify the above findings, we used the reductions of emissions of acid  
 467 gases (46% and 23% for  $\text{NO}_x$  and  $\text{SO}_2$ , respectively, in the whole China) during the

468 COVID-lockdown period as a further scenario (Huang et al., 2021). The model  
469 simulations suggest that the effectiveness of reductions in SIA and PM<sub>2.5</sub> concentrations  
470 by a 50% NH<sub>3</sub> emission reduction further declined in 2020 ( $15 \pm 0.2\%$  for SIA, and  
471  $5.1 \pm 0.2\%$  for PM<sub>2.5</sub>), but the resulting concentrations of them were lower ( $20.8 \pm 0.3\%$   
472 for SIA, and  $15.6 \pm 0.3\%$  for PM<sub>2.5</sub>) when compared with that in 2017 under the same  
473 scenario of an additional 50% NH<sub>3</sub> emissions reduction (and constant meteorological  
474 conditions) (Fig. 6 and Table S6), highlighting the importance of concurrently NH<sub>3</sub>  
475 mitigation when acid gas emissions are strengthened. To confirm the importance of acid  
476 gas emissions, another sensitivity simulation was conducted for 2017, in which the acid  
477 gas (NO<sub>x</sub> and SO<sub>2</sub>) emissions were reduced by 50% (Fig. 7). We found that reductions  
478 in SIA concentrations are  $13.4 \pm 0.5\%$  greater for the 50% reductions in SO<sub>2</sub> and NO<sub>x</sub>  
479 emissions than for the 50% reductions in NH<sub>3</sub> emissions. These results indicate that to  
480 substantially reduce SIA pollution it remains imperative to strengthen emission controls  
481 on NO<sub>x</sub> and SO<sub>2</sub> even when a 50% reduction in NH<sub>3</sub> emission is targeted and achieved.  
482



483  
 484 **Fig. 7.** Left: the spatial distributions of simulated PM<sub>2.5</sub> concentrations (in μg m<sup>-3</sup>) in  
 485 January 2017 with (a) 50% reductions in ammonia (NH<sub>3</sub>) emissions and (b) 50%  
 486 reductions in acid gas (NO<sub>x</sub> and SO<sub>2</sub>) emissions. Right: the % decreases in PM<sub>2.5</sub> (c)  
 487 and SIA (d) concentrations for the simulations with compared to without the NH<sub>3</sub> and  
 488 acid gas emissions reductions in four megacity clusters (BTH: Beijing-Tianjin-Hebei,  
 489 YRD: Yangtze River Delta, SCB: Sichuan Basin, PRD: Pearl River Delta). \*\* denotes  
 490 significant differences without and with 50% ammonia emission reductions (*P* < 0.05).  
 491 *n* is the number of calculated samples by grid extraction. Error bars are standard errors  
 492 of means.

### 493 3.3. Uncertainty analysis and limitations

494 Some limitations should be noted in interpreting the results of the present study: this  
 495 study examined period-to-period changes in PM<sub>2.5</sub> chemical components based on a



496 meta-analysis and the efficiencies of  $\text{NH}_3$  and acid gas emission reductions on  $\text{PM}_{2.5}$   
497 mitigation. Some uncertainties may still exist in meta-analysis of nationwide  
498 measurements owing to differences in monitoring, sample handling and analysis  
499 methods as well as lack of long-term continuous monitoring sites (Fig. 2). For example,  
500 the measurements of  $\text{PM}_{2.5}$  were mainly taken using the TEOM method, which is  
501 associated with under-reading of PM due to some nitrate volatilization at its operational  
502 temperature. To test whether the use of data during 2000–2019 could bias annual trends  
503 of  $\text{PM}_{2.5}$  and chemical components, we summarize measurements of  $\text{PM}_{2.5}$  at a long-  
504 term monitoring site (Quzhou County) during the period 2012–2020. The  $\text{PM}_{2.5}$  and  
505  $\text{SO}_4^{2-}$  show the decreasing trend. The concentration of  $\text{NO}_3^-$  and  $\text{NH}_4^+$  do not show  
506 significant change (Fig. S8). The results are consistent with the trend for the whole of  
507 China obtained from the meta-analysis. Considering the uncertainty of  $\text{PM}_{2.5}$  and its  
508 major components between different seasons (winter, summer, etc) and site type (urban,  
509 suburban or rural). We have analyzed historic trend in the different season and sites  
510 (Figs. S13–S20). We found that concentrations of  $\text{PM}_{2.5}$  and its major chemical  
511 components ( $\text{SO}_4^{2-}$ ,  $\text{NO}_3^-$ , and  $\text{NH}_4^+$ ) were significantly higher in fall and winter than  
512 in spring and summer (Fig. S13). Only the winter season showed significant change  
513 trend in the three periods (Figs. S14–S17). The analyses also confirmed that pollution  
514 days predominated in winter. We also found that concentrations of  $\text{PM}_{2.5}$  and its major  
515 chemical components were higher at urban than rural sites (Fig. S18). Spatially, the  
516 trends of  $\text{PM}_{2.5}$  and its major components are similar across the whole of China (both  
517 of urban and rural) (Fig. S19). Rural areas show the same change trend in hazy days  
518 compared with whole of China (Fig. S20).

519 WRF-CMAQ model performance also has some uncertainty. We performed the  
520 validations of WRF and CMAQ models. The simulations of temperature at 2 m above

521 ground (T2), wind speed (WS), and relative humidity (RH) versus observed values at  
522 400 monitoring sites in China are shown in Fig. S7. The meteorological measurements  
523 were obtained from the National Climate Data Center (NCDC)  
524 (<ftp://ftp.ncdc.noaa.gov/pub/data/noaa/>). The comparisons showed that the model  
525 performed well at predicting meteorological parameters with  $R$  values of 0.94, 0.64 and  
526 0.82 for T2, WS and RH, respectively. However, the WS was overestimated (22.3%  
527 NMB) in most regions of China, which is also reported in previous studies (Gao et al.,  
528 2016; Chen et al., 2019). This may be related to the underlying surface parameters set  
529 in the WRF model configurations.

530 In addition, the simulations of PM<sub>2.5</sub> and associated chemical components by the  
531 CMAQ model have potential biases in the spatial pattern, although the CMAQ model  
532 has been extensively used in air quality studies (Backes et al., 2016; Zhang et al., 2019)  
533 and the validity of the chemical regime in the CMAQ model had been confirmed by  
534 our previous studies (Zhang et al., 2021a; Wang et al., 2020a, 2021a). Since nationwide  
535 measurements of PM<sub>2.5</sub> and associated chemical components are lacking in 2010 in  
536 China, we undertook our own validation of PM<sub>2.5</sub> and its components (such as SO<sub>4</sub><sup>2-</sup>,  
537 NO<sub>3</sub><sup>-</sup>, and NH<sub>4</sub><sup>+</sup>) using a multi-observation dataset that includes those monitoring data  
538 and satellite observations at a regional scale that were available.

539 First, the simulated monthly mean PM<sub>2.5</sub> concentration in January 2010 was  
540 compared with corresponding data obtained from the ChinaHighAirPollutants (CHAP,  
541 <https://weijing-rs.github.io/product.html>) database. The satellite historical PM<sub>2.5</sub>  
542 predictions are reliable (average  $R^2 = 0.80$  and RMSE = 11.26  $\mu\text{g m}^{-3}$ ) using cross  
543 validation against the in-situ surface observations on a monthly basis (Wei et al., 2020,  
544 2021). The model well captured the spatial distributions of PM<sub>2.5</sub> concentrations in our  
545 studied regions of BTH, YRD, PRD, and SCB (Fig. S3a), with correlation coefficient

546 ( $R$ ) between simulated and satellite observed  $\text{PM}_{2.5}$  concentrations of 0.96, 0.80, 0.60,  
547 and 0.85 for BTH, YRD, PRD, and SCB, respectively.

548 Second, we also collected ground-based observations from previous publications  
549 (Xiao et al., 2020, 2021; Geng et al., 2019; Xue et al., 2019) to validate the modeling  
550 concentrations of  $\text{SO}_4^{2-}$ ,  $\text{NO}_3^-$ , and  $\text{NH}_4^+$ . Detailed information about the monitoring  
551 sites is presented in Table S5. The distributions of the simulated monthly mean  
552 concentrations of  $\text{SO}_4^{2-}$ ,  $\text{NO}_3^-$ , and  $\text{NH}_4^+$  in January 2010 over China is compared with  
553 collected surface measurements are shown in Fig. S4a, b, and c, respectively, with their  
554 linear regression analysis presented in Fig. S4d. The model showed underestimation in  
555 simulating  $\text{SO}_4^{2-}$  and  $\text{NO}_3^-$  in the BTH region, which might be caused by the uncertainty  
556 in the emission inventory. The lack of heterogeneous pathways for  $\text{SO}_4^{2-}$  formation in  
557 the CMAQ model might also be an important reason for the negative bias between  
558 simulations and measurements (Yu et al., 2005; Cheng et al., 2016). The model  
559 overestimated  $\text{NO}_3^-$  concentration in the SCB region, but can capture the spatial  
560 distribution of  $\text{NO}_3^-$  in other regions. The overestimation of  $\text{NO}_3^-$  has been a common  
561 problem in regional chemical transport models such as CMAQ, GEOS-CHEM and  
562 CAMx (Yu et al., 2005; Fountoukis et al., 2011; Zhang et al., 2012; Wang et al., 2013),  
563 due to the difficulties in correctly capturing the gas and aerosol-phase nitrate  
564 partitioning (Yu et al., 2005). The modeling of  $\text{NH}_4^+$  concentrations show good  
565 agreement with the observed values. Generally, the evaluation results indicate that the  
566 model reasonably predicted concentrations of  $\text{SO}_4^{2-}$ ,  $\text{NO}_3^-$ , and  $\text{NH}_4^+$  in  $\text{PM}_{2.5}$ .

567 Third, we performed a comparison of the time-series of the observed and simulated  
568 hourly  $\text{PM}_{2.5}$  and its precursors ( $\text{SO}_2$  and  $\text{NO}_2$ ) during January 2010. The model well  
569 captures the temporal variations of the  $\text{PM}_{2.5}$  in Beijing, with an NMB value of  $0.05 \mu\text{g}$   
570  $\text{m}^{-3}$ , NME of 28%, and  $R$  of 0.92 (Fig. 5a). The predicted daily concentrations of  $\text{NO}_2$

571 and SO<sub>2</sub> during January 2010 also show good agreement with the ground measurements  
572 in Beijing, with NMB and *R* values of 0.12 μg m<sup>-3</sup> and 0.89 for NO<sub>2</sub>, and -0.04, 0.95  
573 for SO<sub>2</sub>, respectively (Fig. 5b). The variations of daily PM<sub>2.5</sub> concentrations between  
574 simulation and observation at 4 monitoring sites (Shangdianzi, Chengdu, Institute of  
575 Atmospheric Physics, Chinese Academy of Sciences (IAP-CAS), and Tianjin) from 14  
576 to 30 January 2010 also matched well, with NMB values ranging from -0.05 to 0.12 μg  
577 m<sup>-3</sup>, and *R* values exceeding 0.89 (Fig. S5c).

578 We also compared the simulated and observed concentrations of PM<sub>2.5</sub>, NO<sub>2</sub>, and  
579 SO<sub>2</sub> in China in pre-COVID period (1–26 January 2020) and during the COVID-  
580 lockdown period (27 January–26 February) with actual meteorological conditions. As  
581 shown in Fig. S6, both the simulations and observations suggested that the PM<sub>2.5</sub> and  
582 NO<sub>2</sub> concentrations substantially decreased during the COVID-lockdown, mainly due  
583 to the sharp reduction in vehicle emissions (Huang et al., 2021; Wang et al., 2021b).  
584 For SO<sub>2</sub>, the concentrations decreased very little and even increased at some monitoring  
585 sites. The model underestimated the concentrations of PM<sub>2.5</sub>, NO<sub>2</sub>, and SO<sub>2</sub>, with NMB  
586 values of -21.4%, -22.1%, and -9.6%, respectively. We also newly evaluated the model  
587 performance in actual meteorological conditions for PM<sub>2.5</sub> concentrations in January  
588 2014 and 2017, respectively. As shown in the Figure S21, the model well captured the  
589 spatial distribution of PM<sub>2.5</sub> concentration in China with MB (NMB) values of 23.2 μg  
590 m<sup>-3</sup> (15.4%) and 26.8 μg m<sup>-3</sup> (-26.7%) for 2014 and 2017, respectively. The simulated  
591 PM<sub>2.5</sub> concentrations compared well against the observations, with *R* values of 0.82 and  
592 0.65, respectively

593

594

595

### 596 **3.4. Implication and outlook**

597 Improving air quality is a significant challenge for China and the world. A key  
598 target in China is for all cities to attain annual mean PM<sub>2.5</sub> concentrations of 35 µg m<sup>-3</sup>  
599 or below by 2035 (Xing et al., 2021). However, this study has shown that 74% of 1498  
600 nationwide measurement sites have exceeded this limit value in recent years (averaged  
601 across 2015-2019). Our results indicated that acid gas emissions still need to be a focus  
602 of control measures, alongside reductions in NH<sub>3</sub> emissions, in order to reduce SIA (or  
603 PM<sub>2.5</sub>) formation. Model simulations for the month of January underpin the finding that  
604 the relative effectiveness of NH<sub>3</sub> emission control decreased over the period from 2010  
605 to 2017. However, simulating the substantial emission reductions in acid gases due to  
606 the lockdown during the COVID-19 pandemic, with fossil fuel-related emissions  
607 reduced to unprecedented levels, indicated the importance of ammonia emission  
608 abatement for PM<sub>2.5</sub> air quality improvements when SO<sub>2</sub> and NO<sub>x</sub> emissions have  
609 already reached comparatively low levels. Therefore, a strategic and integrated  
610 approach to simultaneously undertaking acid gas emissions and NH<sub>3</sub> mitigation is  
611 essential to substantially reduce PM<sub>2.5</sub> concentrations. However, the mitigation of acid  
612 gas and NH<sub>3</sub> emissions pose different challenges due to different sources they originate  
613 from.

614 The implementation of further reduction of acid gas emissions is challenging. The  
615 prevention and control of air pollution in China originally focused on the control of acid  
616 gas emissions (Fig. S2). The controls have developed from desulfurization and  
617 denitrification technologies in the early stages to advanced end-of-pipe control  
618 technologies. By 2018, over 90% of coal-fired power plants had installed end-of-pipe  
619 control technologies (CEC, 2020). The potential for further reductions in acid gas  
620 emissions by end-of-pipe technology might therefore be limited. Instead, addressing

621 total energy consumption and the promotion of a transition to clean energy through a  
622 de-carbonization of energy production is expected to be an inevitable requirement for  
623 further reducing PM<sub>2.5</sub> concentrations (Xing et al., 2021). In the context of improving  
624 air quality and mitigating climate change, China is adopting a portfolio of low-carbon  
625 policies to meet its Nationally Determined Contribution pledged in the Paris Agreement.  
626 Studies show that if energy structure adjusts and energy conservation measures are  
627 implemented, SO<sub>2</sub> and NO<sub>x</sub> will be further reduced by 34% and 25% in Co-Benefit  
628 Energy scenario compared to the Nationally Determined Contribution scenario in 2035  
629 (Xing et al., 2021). Although it has been reported that excessive acid gas emission  
630 controls may increase the oxidizing capacity of the atmosphere and increase other  
631 pollution, PM<sub>2.5</sub> concentrations have consistently decreased with previous acid gas  
632 control (Huang et al., 2021). In addition, under the influence of low-carbon policies,  
633 other pollutant emissions will also be controlled. Opportunities and challenges coexist  
634 in the control of acid gas emissions.

635 In contrast to acid gas emissions, NH<sub>3</sub> emissions predominantly come from  
636 agricultural sources. Although the Chinese government has recognized the importance  
637 of NH<sub>3</sub> emissions controls in curbing PM<sub>2.5</sub> pollution, NH<sub>3</sub> emissions reductions have  
638 only been proposed recently as a strategic option and no specific nationwide targets  
639 have yet been implemented (CSC, 2018b). The efficient implementation of NH<sub>3</sub>  
640 reduction options is a major challenge because NH<sub>3</sub> emissions are closely related to  
641 food production, and smallholder farming is still the dominant form of agricultural  
642 production in China. The implementation of NH<sub>3</sub> emissions reduction technologies is  
643 subject to investment in technology, knowledge and infrastructure, and most farmers  
644 are unwilling or economically unable to undertake additional expenditures that cannot  
645 generate financial returns (Gu et al., 2011; Wu et al., 2018b). Therefore, economically

646 feasible options for NH<sub>3</sub> emission controls need to be developed and implemented  
647 nationwide.

648 We propose the following three requirements that need to be met to achieve  
649 effective reductions of SIA concentrations and hence of PM<sub>2.5</sub> concentrations in China.

650 First, binding targets to reduce both NH<sub>3</sub> and acid gas emissions should be set. The  
651 targets should be designed to meet the PM<sub>2.5</sub> standard, and NH<sub>3</sub> concentrations should  
652 be incorporated into the monitoring system as a government assessment indicator. In  
653 this study, we find large differences in PM<sub>2.5</sub> concentration reductions from NH<sub>3</sub>  
654 emissions reduction in the four megacity regions investigated. At a local scale (i.e., city  
655 or county), the limiting factors may vary within a region (Wang et al., 2011). Thus,  
656 local-specific environmental targets should be considered in policy-making.

657 Second, further strengthening of the controls on acid gas emissions are still needed,  
658 especially under the influence of low-carbon policies, to promote emission reductions  
659 and the adjustment of energy structures and conservation. Ultra-low emissions should  
660 be requirements in the whole production process, including point source emissions,  
661 diffuse source emissions, and clean transportation (Xing et al., 2021; Wang et al.,  
662 2021a). The assessment of the impact of ultra-low emissions is provided in Table S7.  
663 In terms of energy structure, it is a requirement to eliminate outdated production  
664 capacity and promote low-carbon new energy generation technologies.

665 Third, a requirement to promote feasible NH<sub>3</sub> reduction options throughout the  
666 whole food production chain, for both crop and animal production. Options include the  
667 following. 1) Reduction of nitrogen input at source achieved, for example, through  
668 balanced fertilization based on crop needs instead of over-fertilization, and promotion  
669 of low-protein feed in animal breeding. 2) Mitigation of NH<sub>3</sub> emissions in food  
670 production via, for example, improved fertilization techniques (such as enhanced-

671 efficiency fertilizer (urease inhibitor products), fertilizer deep application, fertilization-  
672 irrigation technologies (Zhan et al., 2021), and coverage of solid and slurry manure. 3)  
673 Encouragement for the recycling of manure back to croplands, and reduction in manure  
674 discarding and long-distance transportation of manure fertilizer. Options for NH<sub>3</sub>  
675 emissions control are provided in Table S4. Although the focus here has been on  
676 methods to mitigate NH<sub>3</sub> emissions, it is of course critical simultaneously to minimize  
677 N losses in other chemical forms such as nitrous oxide gas emissions and aqueous  
678 nitrate leaching (Shang et al., 2019; Wang et al., 2020b).

#### 679 **4. Conclusions**

680 The present study developed an integrated assessment framework using meta-  
681 analysis of published literature results, analysis of national monitoring data, and  
682 chemical transport modelling to provide insight into the effectiveness of SIA precursor  
683 emissions controls in mitigating poor PM<sub>2.5</sub> air quality in China. We found that PM<sub>2.5</sub>  
684 concentration significantly decreased in 2000-2019 due to acid gas control policies, but  
685 PM<sub>2.5</sub> pollution still severe. Compared with other components, this difference was more  
686 significant higher (average increase 98%) for secondary inorganic ions (i.e., SO<sub>4</sub><sup>2-</sup>, NO<sub>3</sub><sup>-</sup>,  
687 and NH<sub>4</sub><sup>+</sup>) on hazy days than on-hazy days. This is mainly caused by the persistent SIA  
688 pollution during the same period. with sulfate concentrations significantly decreased  
689 and no significant changes observed for nitrate and ammonium concentrations. The  
690 reductions of SIA concentrations in January in megacity clusters of eastern China by  
691 additional 50% NH<sub>3</sub> emission controls decreased from 25.9 ± 0.3% in 2010 to 22.9 ±  
692 0.3% in 2017, and to 15 ± 0.2% in the COVID lockdown in 2020 for simulations  
693 representing reduced acid gas emissions to unprecedented levels, but the SIA  
694 concentrations decreased by 20.8 ± 0.3% in 2020 compared with that in 2017 under the  
695 same scenario of an additional 50% NH<sub>3</sub> emissions reduction. In addition, the reduction



696 of SIA concentration in 2017 was  $13.4 \pm 0.5\%$  greater for 50% acid gas ( $\text{SO}_2$  and  $\text{NO}_x$ )  
697 reductions than for the  $\text{NH}_3$  emissions reduction. These results indicate that acid gas  
698 emissions need to be further controlled concertedly with  $\text{NH}_3$  reductions to substantially  
699 reduce  $\text{PM}_{2.5}$  pollution in China.

700 Overall, this study provides new insight into the responses of SIA concentrations  
701 in China to past air pollution control policies and the potential balance of benefits in  
702 including  $\text{NH}_3$  emissions reductions with acid gas emissions controls to curb SIA  
703 pollution. The outcomes from this study may also help other countries seeking feasible  
704 strategies to mitigate  $\text{PM}_{2.5}$  pollution.

705

706

#### 707 **Data availability**

708 All data in this study are available from the from the corresponding authors (Wen Xu,  
709 [wenxu@cau.edu.cn](mailto:wenxu@cau.edu.cn); Shaocai Yu, [shaocaiyu@zju.edu.cn](mailto:shaocaiyu@zju.edu.cn)) upon request.

#### 710 **Author contributions**

711 W.X., S.Y., and F.Z. designed the study. F.M., Y.Z., W.X., and J.K. performed the  
712 research. F.M., Y.Z., W.X., and J.K. analyzed the data and interpreted the results. Y.Z.  
713 conducted the model simulations. L.L. provided satellite-derived surface  $\text{NH}_3$   
714 concentration. F.M., W.X., Y.Z., and M.R.H. wrote the paper, S. R., M.W., K.W., J.K.,  
715 Y.Z., Y.H., P.L., J.W., Z.C., X.L., M.R.H., S.Y. and F.Z. contributed to the discussion  
716 and revision of the paper.

#### 717 **Declaration of Competing Interest**

718 The authors declare that they have no known competing financial interests or personal  
719 relationships that could have appeared to influence the work reported in this paper.

720 **Acknowledgments**

721 This study was supported by National Natural Science Foundation of China (42175137,  
722 21577126 and 41561144004), China Scholarship Council (201913043), the National  
723 Key Research and Development Program of China (2021YFD1700900), the  
724 Department of Science and Technology of China (2016YFC0202702,  
725 2018YFC0213506 and 2018YFC0213503), National Research Program for Key Issues  
726 in Air Pollution Control in China (DQGG0107), and the High-level Team Project of  
727 China Agricultural University. SR's contribution was supported by the Natural  
728 Environment Research Council award number NE/R000131/1 as part of the SUNRISE  
729 program delivering National Capability. We would like to thank Prof. Yuepeng Pan and  
730 Dr. Yangyang Zhang for their help on validating the modeling results.

731 **References**

- 732 An, Z. S., Huang, R. J., Zhang, R. Y., Tie, X. X., Li, G. H., Cao, J. J., Zhou, W. J., Shi,  
733 Z. G., Han, Y. M., Gu, Z. L., and Ji, Y. M.: Severe haze in northern China: A  
734 synergy of anthropogenic emissions and atmospheric processes, *Proc. Natl. Acad.*  
735 *Sci. U. S. A.*, 116, 8657-8666. <https://doi.org/10.1073/pnas.1900125116>, 2019.
- 736 Backes, A., Aulinger, A., Bieser, J., Matthias, V., and Quante, M.: Ammonia emissions  
737 in Europe, part II: How ammonia emission abatement strategies affect secondary  
738 aerosols, *Atmos. Environ.*, 126, 153-161,  
739 <https://doi.org/10.1016/j.atmosenv.2015.11.039>, 2016.
- 740 Bai, Z., Winiwarter, W., Klimont, Z., Velthof, G., Misselbrook, T., Zhao, Z., Jin, X.,  
741 Oenema, O., Hu, C., and Ma, L.: Further improvement of air quality in China needs  
742 clear ammonia mitigation target, *Environ. Sci. Technol.*, 53, 10542-10544,  
743 <https://doi.org/10.1021/acs.est.9b04725>, 2019.
- 744 Benitez-Lopez, A., Alkemade, R., Schipper, A. M., Ingram, D. J., Verweij, P. A.,

745 Eikelboom, J. A. J., and Huijbregts, M. A. J.: The impact of hunting on tropical  
746 mammal and bird populations, *Science*, 356, 180-183, [https://doi.org/](https://doi.org/10.1126/science.aaj1891)  
747 [10.1126/science.aaj1891](https://doi.org/10.1126/science.aaj1891), 2017.

748 Bracken, M. B.: Statistical methods for analysis of effects of treatment in overviews of  
749 randomized trials. In: J.C. Sinclair, M.B. Bracken (Eds.) *Effective care of the*  
750 *newborn infant*, Oxford University Press, 1992.

751 Chen, Z.Y., Chen, D.L., Wen, W., Zhuang, Y., Kwan, M.P., Chen, B., Zhao, B., Yang,  
752 L., Gao, B.B., Li, R.Y., and Xu, B.: Evaluating the “2+26” regional strategy for air  
753 quality improvement during two air pollution alerts in Beijing: Variations in PM<sub>2.5</sub>  
754 concentrations, source apportionment, and the relative contribution of local  
755 emission and regional transport, *Atmos. Chem. Phys.*, 19, 6879-6891.  
756 <https://doi.org/10.5194/acp-19-6879-2019>, 2019.

757 Cheng, Y.F., Zheng, G.A., Wei, C., Mu, Q., Zheng, B., Wang, Z.B., Gao, M., Zhang, Q.,  
758 He, K.B., Carmichael, G., Poschl, U., and Su, H.: Reactive nitrogen chemistry in  
759 aerosol water as a source of sulfate during haze events in China, *Sci. Adv.* 2(12).  
760 <https://doi.org/10.1126/sciadv.1601530>, 2016.

761 China Electricity Council.: *China Power Industry Annual Development Report 2019*,  
762 <https://www.cec.org.cn/yaowenkuaidi/2019-06-14/191782.html>, 2020.

763 CSC (China State Council): *The 11th Five-Year plan on energy saving and emissions*  
764 *reduction*, [http://www.gov.cn/zhengce/content/2008-03/28/content\\_4877.htm](http://www.gov.cn/zhengce/content/2008-03/28/content_4877.htm),  
765 2007.

766 CSC (China State Council): *The 12th Five-Year plan on energy saving and emissions*  
767 *reduction*. [http://www.gov.cn/zwggk/2011-12/20/content\\_2024895.htm](http://www.gov.cn/zwggk/2011-12/20/content_2024895.htm), 2011.

768 CSC (China State Council): *Action Plan on Prevention and Control of Air Pollution*,  
769 China State Council, Beijing, China. <http://www.gov.cn/zwggk/2013->

770 09/12/content\_2486773.htm, 2013.

771 CSC (China State Council): The 13th Five-Year plan on energy saving and emissions  
772 reduction. [http://www.gov.cn/zhengce/content/2016-12/05/content\\_5143290.htm](http://www.gov.cn/zhengce/content/2016-12/05/content_5143290.htm),  
773 2016.

774 CSC (China State Council): Air quality targets set by the Action Plan have been fully  
775 realized, [http://www.gov.cn/xinwen/2018-02/01/content\\_5262720.htm](http://www.gov.cn/xinwen/2018-02/01/content_5262720.htm), 2018a.

776 CSC (China State Council): Notice of the state council on issuing the three-year action  
777 plan for winning the Blue Sky defense battle.  
778 [http://www.gov.cn/zhengce/content/2018-07/03/content\\_5303158.htm](http://www.gov.cn/zhengce/content/2018-07/03/content_5303158.htm), 2018b.

779 Dunn, O.J.: Multiple comparisons using rank sums. *Technometrics*, 6, 241-252, 1964.

780 Fountoukis, C., Racherla, P. N., Denier van der Gon, H. A. C., Polymeneas, P.,  
781 Charalampidis, P. E., Pilinis, C., Wiedensohler, A., Dall'Osto, M., O'Dowd, C., and  
782 Pandis, S. N.: Evaluation of a three-dimensional chemical transport model  
783 (PMCAMx) in the European domain during the EUCAARI May 2008 campaign,  
784 *Atmos. Chem. Phys.*, 11, 10331–10347, [https://doi.org/10.5194/acp-11-10331-](https://doi.org/10.5194/acp-11-10331-2011)  
785 2011, 2011.

786 Fan, C., Li, Z., Li, Y., Dong, J., van der A, R., and de Leeuw, G.: Variability of NO<sub>2</sub>  
787 concentrations over China and effect on air quality derived from satellite and  
788 ground-based observations, *Atmos. Chem. Phys.*, 21, 7723-7748,  
789 <https://doi.org/10.5194/acp-21-7723-2021>, 2021.

790 Feng, S. J., Xu, W., Cheng, M. M., Ma, Y. X., Wu, L. B., Kang, J. H., Wang, K., Tang,  
791 A. H., Collett Jr., J. L., Fang, Y. T., Goulding, K., Liu, X. J., and Zhang, F. S.:  
792 Overlooked nonagricultural and wintertime agricultural NH<sub>3</sub> emissions in Quzhou  
793 County, North China Plain: Evidence from <sup>15</sup>N-stable isotopes, *Environ. Sci.*  
794 *Technol. Lett.*, 9, 127-133, <https://doi.org/10.1021/acs.estlett.1c00935>, 2022.

795 Gao, M., Carmichael, G. R., Wang, Y., Saide, P. E., Yu, M., Xin, J., Liu, Z., and Wang,  
796 Z.: Modeling study of the 2010 regional haze event in the North China Plain, *Atmos.*  
797 *Chem. Phys.*, 16, 1673–1691, <https://doi.org/10.5194/acp-16-1673-2016>, 2016.

798 Geng, G., Xiao, Q., Zheng, Y., Tong, D., Zhang, Y., Zhang, X., Zhang, Q., He, K., and  
799 Liu, Y.: Impact of China’s air pollution prevention and control action plan on PM<sub>2.5</sub>  
800 chemical composition over eastern China, *Sci China Earth Sci.*, 62, 1872-1884,  
801 <https://doi.org/10.1007/s11430-018-9353-x>, 2019.

802 Geng, G., Xiao, Q., Liu, S., Liu, X., Cheng, J., Zheng, Y., Xue, T., Tong, D., Zheng,  
803 B., Peng, Y., and Huang, X.: Tracking air pollution in China: Near real-time PM<sub>2.5</sub>  
804 retrievals from multisource data fusion, *Environ. Sci. Technol.*, 55, 12106-12115,  
805 <https://doi.org/10.1021/acs.est.1c01863>, 2021.

806 Geng, G., Zhang, Q., Tong, D., Li, M., Zheng, Y., Wang, S., and He, K.: Chemical  
807 composition of ambient PM<sub>2.5</sub> over China and relationship to precursor emissions  
808 during 2005–2012, *Atmos. Chem. Phys.*, 17, 9187–9203,  
809 <https://doi.org/10.5194/acp-17-9187-2017>, 2017.

810 Gu, B. J., Zhu, Y. M., Chang, J., Peng, C. H., Liu, D., Min, Y., Luo, W. D., Howarth, R.  
811 W., and Ge, Y.: The role of technology and policy in mitigating regional nitrogen  
812 pollution, *Environ. Res. Lett.*, 6, 1, <https://doi.org/10.1088/1748-9326/6/1/014011>,  
813 2011.

814 Guenther, A. B., Jiang, X., Heald, CL., Sakulyanontvittaya, T., Duhl, T., Emmons, L.  
815 K., and Wang, X.: The Model of Emissions of Gases and Aerosols from Nature  
816 version 2.1 (MEGAN2.1): an extended and updated framework for modeling  
817 biogenic emissions, *Geosci. Model Dev.*, 5, 1471-1492.  
818 <https://doi.org/10.5194/gmd-5-1471-2012>, 2012.

819 Han, Y., Wu, Y. F., Don, H. Y., and Chen, F.: Characteristics of PM<sub>2.5</sub> and its chemical

820 composition during the Asia-Pacific Economic Cooperation Summit in Beijing-  
821 Tianjin-Hebei Region and surrounding cities, *Environ. Sci. Technol.*, 40, 134-138  
822 (in Chinese with English abstract), 2017.

823 Huang, R. J., Zhang, Y. L., Bozzetti, C., Ho, K. F., Cao, J. J., Han, Y. M., Daellenbach,  
824 K. R., Slowik, J. G., Platt, S. M., Canonaco, F., Zotter, P., Wolf, R., Pieber, S. M.,  
825 Bruns, E. A., Crippa, M., Ciarelli, G., Piazzalunga, A., Schwikowski, M.,  
826 Abbaszade, G., Schnelle-Kreis, J., Zimmermann, R., An, Z. S., Szidat, S.,  
827 Baltensperger, U., El Haddad, I., and Prevot, A. S.: High secondary aerosol  
828 contribution to particulate pollution during haze events in China, *Nature*, 514, 218-  
829 222. <https://doi.org/10.1038/nature13774>, 2014.

830 Huang, X., Ding, A.J, Gao, J., Zheng, B., Zhou, D.R., Qi, X. M., Tang, R., Wang, J. P.,  
831 Ren, C. H., Nie, W., Chi, X. G., Xu, Z., Chen, L. D., Li, Y. Y., Che, F., Pang, N. N.,  
832 Wang, H. K., Tong, D., Qin, W., Cheng, W., Liu, W. J., Fu, Q. Y., Liu, B. X., Chai,  
833 F. H., Davis, S. J., Zhang, Q., and He, K. B.: Enhanced secondary pollution offset  
834 reduction of primary emissions during COVID-19 lockdown in China, *Natl. Sci.*  
835 *Rev.*, 8, 137, <https://doi.org/10.1093/nsr/nwaa137>, 2021.

836 Ianniello, A., Spataro, F., Esposito, G., Allegrini, I., Rantica, E., Ancora, MP., Hu, M.,  
837 and Zhu, T.: Occurrence of gas phase ammonia in the area of Beijing (China).  
838 *Atmos. Chem. Phys.*, 10, 9487-9503, <https://doi.org/10.5194/acp-10-9487-2010>, 2010.

839 Kang, Y. N., Liu, M. X., Song, Y., Huang, X., Yao, H., Cai, X. H., Zhang, H. S., Kang,  
840 L., Liu, X. J., Yan, X. Y., He, H., Zhang, Q., Shao, M., and Zhu, T.: High-resolution  
841 ammonia emissions inventories in China from 1980 to 2012, *Atmos. Chem. Phys.*,  
842 16, 2043-2058, <https://doi.org/10.5194/acp-16-2043-2016>, 2016.

843 Kruskal, W.H. and Wallis, W.A.: Use of ranks in one-criterion variance  
844 analysis. *Journal of the American statistical Association*, 47, 583-621,

845 <https://doi.org/10.1080/01621459.1952.10483441>, 1952.

846 Kuerban, M., Waili, Y., Fan, F., Liu, Y., Qin, W., Dore, A. J., Dore, A. J., Xu, W., and  
847 Zhang, F. S.: Spatio-temporal patterns of air pollution in China from 2015 to 2018  
848 and implications for health risks, *Environ. Pollut.*, 258, 113659, [https://doi.org/](https://doi.org/10.1016/j.envpol.2019.113659)  
849 [10.1016/j.envpol.2019.113659](https://doi.org/10.1016/j.envpol.2019.113659), 2020.

850 Li, H., Cheng, J., Zhang, Q., Zheng, B., Zhang, Y., Zheng, G., and He, K.: Rapid  
851 transition in winter aerosol composition in Beijing from 2014 to 2017: response to  
852 clean air actions, *Atmos. Chem. Phys.*, 19, 11485–11499,  
853 <https://doi.org/10.5194/acp-19-11485-2019>, 2019.

854 Li, H. Y., Zhang, Q., Zheng, B., Chen, C. R., Wu, N. N., Guo, H. Y., Zhang, Y. X., Zheng,  
855 Y. X., Li, X., and He, K. B.: Nitrate-driven urban haze pollution during summertime  
856 over the North China Plain, *Atmos. Chem. Phys.*, 18, 5293-5306, [https://doi.org/](https://doi.org/10.5194/acp-18-5293-2018)  
857 [10.5194/acp-18-5293-2018](https://doi.org/10.5194/acp-18-5293-2018), 2018.

858 Li, K., Jacob, D. J., Shen, L., Lu, X., De Smedt, I., and Liao, H.: Increases in surface  
859 ozone pollution in China from 2013 to 2019: anthropogenic and meteorological  
860 influences, *Atmos. Chem. Phys.*, 20, 11423–11433, [https://doi.org/10.5194/acp-20-](https://doi.org/10.5194/acp-20-11423-2020)  
861 [11423-2020](https://doi.org/10.5194/acp-20-11423-2020), 2020.

862 Li, M., Liu, H., Geng, G., Geng, G. N., Hong, C. P., Liu, F., Song, Y., Tong, D., Zheng,  
863 B., Cui, H. Y., Man, H. Y., Zhang, Q., and He, K. B.: Anthropogenic emission  
864 inventories in China: a review, *Natl. Sci. Rev.*, 4, 834-866.  
865 <https://doi.org/10.1093/nsr/nwx150>, 2017.

866 Li, X., Bei, N., Hu, B., Wu, J., Pan, Y., Wen, T., Liu, Z., Liu, L., Wang, R., and Li, G.:  
867 Mitigating NO<sub>x</sub> emissions does not help alleviate wintertime particulate pollution  
868 in Beijing-Tianjin-Hebei, China, *Environ. Pollut.*, 279(X), [https://](https://doi.org/10.1016/j.envpol.2021.11693)  
869 [10.1016/j.envpol.2021.11693](https://doi.org/10.1016/j.envpol.2021.11693), 2021.

870 Liang, F. C., Xiao, Q. Y., Huang, K. Y., Yang, X. L., Liu, F. C., Li, J. X., Lu, X. F., Liu,  
871 Y., and Gu, D. F.: The 17-y spatiotemporal trend of PM<sub>2.5</sub> and its mortality burden  
872 in China, *Proc. Natl. Acad. Sci. U. S. A.*, 117, 25601-25608, [https://doi.org/  
873 10.1073/pnas.1919641117](https://doi.org/10.1073/pnas.1919641117), 2020.

874 Liu, J., Han, Y. Q., Tang, X., Zhu, J., and Zhu, T.: Estimating adult mortality attributable  
875 to PM<sub>2.5</sub> exposure in China with assimilated PM<sub>2.5</sub> concentrations based on a ground  
876 monitoring network, *Sci. Total. Environ.*, 568, 1253-1262, [https://doi.org/  
877 10.1016/j.scitotenv.2016.05.165](https://doi.org/10.1016/j.scitotenv.2016.05.165), 2016.

878 Liu, L., Zhang, X. Y., Wong, A. Y. H., Xu, W., Liu, X. J., Li, Y., Mi, H., Lu, X. H., Zhao,  
879 L. M., Wang, Z., Wu, X. D., and Wei, J.: Estimating global surface ammonia  
880 concentrations inferred from satellite retrievals, *Atmos. Chem. Phys.*, 19, 12051-  
881 12066, <https://doi.org/10.5194/acp-19-12051-2019>, 2019a.

882 Liu, M. X., Huang, X., Song, Y., Tang, J., Cao, J. J., Zhang, X. Y., Zhang, Q., Wang, S.  
883 X., Xu, T. T., Kang, L., Cai, X. H., Zhang, H. S., Yang, F. M., Wang, H. B., Yu, J.  
884 Z., Lau, A. K. H., He, L. Y., Huang, X. F., Duan, L., Ding, A. J., Xue, L. K., Gao,  
885 J., Liu, B., and Zhu, T.: Ammonia emission control in China would mitigate haze  
886 pollution and nitrogen deposition, but worsen acid rain, *Proc. Natl. Acad. Sci. U. S.*  
887 *A.*, 116, 7760-7765, <https://doi.org/10.1073/pnas.1814880116>, 2019b.

888 Liu, X.J., Sha, Z.P., Song, Y., Dong, H.M., Pan, Y.P., Gao, Z.L., Li, Y.E., Ma, L., Dong,  
889 W.X., Hu, C.S., Wang, W.L., Wang, Y., Geng, H., Zheng, Y.H., and Gu, M.N.:  
890 China's atmospheric ammonia emission characteristics, mitigation options and  
891 policy recommendations, *Res. Environ. Sci.*, 34, 149-157,  
892 <https://10.13198/j.issn.1001-6929.2020.11.12>, 2021.

893 Mao, S. S., Chen, T, Fu, J. M., Liang, J. L., An, X. X., Luo, X. X., Zhang, D. W., and



894 Liu, B. X.: Characteristic analysis for the thick winter air pollution accidents in  
895 Beijing based on the online observations, *Journal of Safety and Environment*. 1,  
896 1009-6094 ( in Chinese with English abstract), 2018.

897 MEEP. The Ministry of Ecology and Environment of the People's Republic of China,  
898 China Ecological Environment Bulletin.  
899 <http://www.mee.gov.cn/hjzl/sthjzk/zghjzkgb/>, 2019.

900 Megaritis, A., Fountoukis, C., Charalampidis, P. E., Pilinis, C., and Pandis, S. N.:  
901 Response of fine particulate matter concentrations to changes of emissions and  
902 temperature in Europe, *Atmos. Chem. Phys.*, 13, 3423-3443,  
903 <https://doi.org/10.5194/acp-13-3423-2013>, 2013.

904 Meng, F. L., Wang, M. R., Stokal, M., Kroeze, C., Ma, L., Li, Y. N., Zhang, Q., Wei,  
905 Z. B., Hou, Y., Liu, X. J., Xu, W., and Zhang, F. S.: Nitrogen losses from food  
906 production in the North China Plain: A case study for Quzhou, *Sci. Total. Environ.*,  
907 816, 151557, <https://doi.org/10.1016/j.scitotenv.2021.151557>, 2022.

908 MEPC. Ministry of Environment Protection of China, Ambient air quality standards  
909 (GB3095–2012). <http://www.mep.gov.cn/>, 2012.

910 Morrison, H., Thompson, G., and Tatarskii, V.: Impact of cloud microphysics on the  
911 development of trailing stratiform precipitation in a simulated squall line:  
912 comparison of one- and two-moment schemes, *Mon. Weather. Rev.*, 137, 991-1007.  
913 <https://doi.org/10.1175/2008MWR2556.1>, 2012 .

914 Nakagawa, S. and Santos, E. S. A.: Methodological issues and advances in biological  
915 meta-analysis, *Evol. Ecol.*, 26, 1253-1274. [https://doi.org/10.1007/s10682-012-](https://doi.org/10.1007/s10682-012-9555-5)  
916 9555-5, 2012.

917 Ortiz-Montalvo, D. Häkkinen, S. A. K., Schwier, A. N., Lim, Y. B., Faye McNeill, V.,  
918 and Turpin, B. J.: Ammonium addition (and aerosol pH) has a dramatic impact on

919 the volatility and yield of glyoxal secondary organic aerosol, *Environ. Sci. Technol.*,  
920 48, 255-262, <https://doi.org/10.1021/es4035667>, 2014.

921 Pan, Y. P., Wang, Y. S., Tang, G. Q., and Wu, D.: Wet and dry deposition of atmospheric  
922 nitrogen at ten sites in Northern China, *Atmos. Chem. Phys.*, 12, 6515–6535,  
923 doi:10.5194/acp-12-6515-2012, 2012.

924 Pinder, R. W., Adams, P. J., and Pandis, S. N.: Ammonia emission controls as a cost-  
925 effective strategy for reducing atmospheric particulate matter in the eastern United  
926 States, *Environ. Sci. Technol.*, 41, 380-386, <https://doi.org/10.1021/es060379a>,  
927 2007.

928 Ronald, J. V., Mijling, B., Ding, J. Y., Koukouli, M. E., Liu, F., Li, Q., Mao, H. Q., and  
929 Theys, N.: Cleaning up the air: effectiveness of air quality policy for SO<sub>2</sub> and NO<sub>x</sub>  
930 emissions in China, *Atmos. Chem. Phys.*, 17, 1775-1789,  
931 <https://doi.org/10.5194/acp-17-1775-2017>, 2017.

932 Shang, Z.Y., Zhou, F., Smith, P., Saikawa, E., Ciais, P., Chang, J.F., Tian, H.Q., Del  
933 Grosso, S.L., Ito, A., Chen, M.P., Wang, Q.H., Bo, Y., Cui, X.Q., Castaldi, S.,  
934 Juszczak, P., Kasimire, A., Magliulo, V., Medinets, S., Medinets, V., Rees, R. M.,  
935 Wohlfahrt, G., and Sabbatini, S: Weakened growth of cropland-N<sub>2</sub>O emissions in  
936 China associated with nationwide policy interventions, *Glob. Change. Biol.*, 25,  
937 3706-3719, <https://doi.org/10.1111/gcb.14741>, 2021.

938 Sun, Y. L., Zhuang, G. S., Tang, A. H., Wang, Y., and An, Z. S.: Chemical characteristics  
939 of PM<sub>2.5</sub> and PM<sub>10</sub> in haze-fog episodes in Beijing, *Environ. Sci. Technol.*, 40, 3148-  
940 3155, <https://doi.org/10.1021/es051533g>, 2006.

941 Tao, J., Gao, J., Zhang, L. M., Wang, H., Qiu, X. H., Zhang, Z. S., Wu, Y. F., Chai, F.  
942 H., and Wang, S. L: Chemical and optical characteristics of atmospheric aerosols in  
943 Beijing during the Asia-Pacific Economic Cooperation China 2014, *Atmos.*

944 Environ., 144, 8-16, <https://doi.org/10.1016/j.atmosenv.2016.08.067>, 2016.

945 Wang S.: How to promote ultra-low emissions during the 14th Five-Year Plan? China.  
946 Environment. News. [http://epaper.cenews.com.cn/html/2021-04/30/node\\_7.htm](http://epaper.cenews.com.cn/html/2021-04/30/node_7.htm),  
947 2021a.

948 Wang, G. H., Zhang, R. Y., Gomez, M. E., Yang, L. X., Zamora, M. L., Hu, M., Lin, Y.,  
949 Peng, J. F., Guo, S., Meng, J. J., Li, J. J., Cheng, C. L., Hu, T. F., Ren, Y. Q., Wang,  
950 Y. S., Gao, J., Cao, J. J., An, Z. S., Zhou, W. J., Li, G. H., Wang, J. Y., Tian, P. F.,  
951 Marrero-Ortiz, W., Secretst, J., Du, Z. F., Zheng, J., Shang, D. J., Zeng, L. M., Shao,  
952 M., Wang, W. G., Huang, Y., Wang, Y., Zhu, Y. J., Li, Y. X., Hu, J. X., Pan, B., Cai,  
953 L., Cheng, Y. T., Ji, Y. M., Zhang, F., Rosenfeld, D., Liss, P. S., Duce, R. A., Kolb,  
954 C. E., and Molina, M. J.: Persistent sulfate formation from London Fog to Chinese  
955 haze, *Proc. Natl. Acad. Sci. U. S. A.*, 113, 13630-13635, [https://doi.org/](https://doi.org/10.1073/pnas.1616540113)  
956 [10.1073/pnas.1616540113](https://doi.org/10.1073/pnas.1616540113), 2016.

957 Wang, L., Chen, X., Zhang, Y., Li, M., Li, P., Jiang, L., Xia, Y., Li, Z., Li, J., Wang, L.,  
958 Hou, T., Liu, W., Rosenfeld, D., Zhu, T., Zhang, Y., Chen, J., Wang, S., Huang, Y.,  
959 Seinfeld, J. H., and Yu, S.: Switching to electric vehicles can lead to significant  
960 reductions of PM<sub>2.5</sub> and NO<sub>2</sub> across China, *One Earth*, 4, 1037–1048,  
961 <https://doi.org/10.1016/j.oneear.2021.06.008>, 2021b.

962 Wang, L., Yu, S., Li, P., Chen, X., Li, Z., Zhang, Y., Li, M., Mehmood, K., Liu, W., Chai,  
963 T., Zhu, Y., Rosenfeld, D., and Seinfeld, J. H.: Significant wintertime PM<sub>2.5</sub>  
964 mitigation in the Yangtze River Delta, China, from 2016 to 2019: observational  
965 constraints on anthropogenic emission controls, *Atmos. Chem. Phys.*, 2, 14787–  
966 14800, <https://doi.org/10.5194/acp-20-14787-2020>, 2020a.

967 Wang, Q.H., Zhou, F., Shang, Z.Y., Ciais, P., Winiwarter, W., Jackson, R. B., Tubiello,  
968 F.N., Janssens-Maenhout, G., Tian, H. Q., Cui, X. Q., Canadell, J.G., Piao, S. L.,

969 and Tao, S.: Data-driven estimates of global nitrous oxide emissions from cropland,  
970 Natl. Sci. Rev., 7, 441-452, <https://doi.org/10.1093/nsr/nwz087>, 2020b.

971 Wang, S. X., Xing, J., Jang, C., Jang, C. R., Zhu, Y., Fu, J. S., and Hao, J. M.: Impact  
972 assessment of ammonia emissions on inorganic aerosols in East China using  
973 response surface modeling technique, Environ. Sci. Technol., 45, 9293-9300,  
974 <https://doi.org/10.1021/es2022347>, 2011.

975 Wang, Y. H., Wang, Y. S., Wang, L.L., Petaja, T., Zha, Q.Z., Gong, C.S., Li, S.X., Pan,  
976 Y. P., Hu, B., Xin, J. Y., and Kulmala, M.: Increased inorganic aerosol fraction  
977 contributes to air pollution and haze in China, Atmos. Chem. Phys., 19, 5881-5888.  
978 <https://doi.org/10.5194/acp-19-5881-2019>, 2019a.

979 Wang, Y., Zhang, Q. Q., He, K.B., Zhang, Q., and Chai, L.: Sulfate-nitrate-ammonium  
980 aerosols over China: Response to 2000-2015 emission changes of sulfur dioxide,  
981 nitrogen oxides, and ammonia, Atmos. Chem. Phys., 13, 2635-2652.  
982 <https://doi.org/10.5194/acp-13-2635-2013>, 2013.

983 Wang, Y.C., Chen, J., Wang, Q.Y., Qin, Q.D., Ye, J.H., Han, Y.M., Li, L., Zhen, W., Zhi,  
984 Q., Zhang, Y.X., and Cao, J.J.: Increased secondary aerosol contribution and  
985 possible processing on polluted winter days in China, Environ. Int, 127.  
986 <https://doi.org/10.1016/j.envint.2019.03.021>, 2019b.

987 Wei, J., Li, Z. Q., Cribb, M., Huang, W., Xue, W.H., Sun, L., Guo, J. P., Peng, Y. R., Li,  
988 J., and Lyapustin, A.: Improved 1 km resolution PM<sub>2.5</sub> estimates across China using  
989 enhanced space-time extremely randomized trees, Atmos. Chem. Phys., 20, 3273-  
990 3289. <https://doi.org/10.5194/acp-20-3273-2020>, 2020.

991 Wei, J., Li, Z. Q., Lyapustin, A., Sun, L., Peng, Y. R., Xue, W. H., Su, T. N., and Cribb,  
992 M.: Reconstructing 1-km-resolution high-quality PM<sub>2.5</sub> data records from 2000 to  
993 2018 in China: spatiotemporal variations and policy implications, Remote. Sens.

994 Environ., 252, 112136, <https://doi.org/10.1016/j.rse.2020.112136>, 2021.

995 Wu, Y. J., Wang, P., Yu, S. C., Wang, L. Q., Li, P. F., Li, Z., Mehmood, K., Liu, W. P.,  
996 Wu, J., Lichtfouse, E., Rosenfeld, D., and Seinfeld, J. H.: Residential emissions  
997 predicted as a major source of fine particulate matter in winter over the Yangtze  
998 River Delta, China, Environ. Chem. Lett., 16, 1117-1127.  
999 <https://doi.org/10.1007/s10311-018-0735-6>, 2018a.

1000 Wu, Y. Y., Xi, X. C., Tang, X., Luo, D. M., Gu, B. J., Lam, S. K., Vitousek, P. M., and  
1001 Chen, D. L.: Policy distortions, farm size, and the overuse of agricultural chemicals  
1002 in China, Proc. Natl. Acad. Sci. U. S. A., 115, 7010-7015.  
1003 <https://doi.org/10.1073/pnas.1806645115>, 2018b.

1004 Xiao, Q.Y, Geng, G.N., Liang, F.C., Wang, X., Lv, Z., Lei, Y., Huang, X.M., Zhang, Q.,  
1005 Liu, Y., and He, K.B: Changes in spatial patterns of PM<sub>2.5</sub> pollution in China 2000–  
1006 2018: Impact of clean air policies, Environ. Int., 141, 105776, [https://doi.org/](https://doi.org/10.1016/j.envint.2020.105776)  
1007 [10.1016/j.envint.2020.105776](https://doi.org/10.1016/j.envint.2020.105776), 2020.

1008 Xiao, Q.Y., Zheng, Y.X., Geng, G.N., Chen, C.H., Huang, X.M., Che, H.Z., Zhang, X.Y.,  
1009 He, K.B., and Zhang, Q.: Separating emission and meteorological contribution to  
1010 PM<sub>2.5</sub> trends over East China during 2000–2018, Atmos. Chem. Phys., 21, 9475-  
1011 9496, <https://doi.org/10.5194/acp-21-9475-2021>, 2021.

1012 Xing, J., Liu, X., Wang, S. X., Wang, T., Ding, D., Yu, S., Shindell, D., Ou, Y.,  
1013 Morawska, L., Li, S. W., Ren, L., Zhang, Y. Q., Loughlin, D., Zheng, H. T., Zhao,  
1014 B., Liu, S. C., Smith, K. R., and Hao, J. M.: The quest for improved air quality may  
1015 push China to continue its CO<sub>2</sub> reduction beyond the Paris Commitment, Proc. Natl.  
1016 Acad. Sci. U. S. A., 117, 29535-29542, <https://doi.org/10.1073/pnas.2013297117>,  
1017 2021.

1018 Xu, Q. C., Wang, S. X., Jiang, J. K., Bhattarai, N., Li, X. X., Chang, X., Qiu, X. H.,

1019 Zheng, M., Hua, Y., and Hao, J. M.: Nitrate dominates the chemical composition of  
1020 PM<sub>2.5</sub> during haze event in Beijing, China, *Sci. Total. Environ.*, 689, 1293-1303,  
1021 <https://doi.org/10.1016/j.scitotenv.2019.06.294>, 2019.

1022 Xu, W., Wu, Q.H., Liu, X.J., Tang, A.H., Dore, A.J., and Heal, M.R.: Characteristics of  
1023 ammonia, acid gases, and PM<sub>2.5</sub> for three typical land-use types in the North China  
1024 Plain, *Environ Sci Pollut R.*, 23, 1158-1172. [https://doi.org/10.1007/s11356-015-](https://doi.org/10.1007/s11356-015-5648-3)  
1025 [5648-3](https://doi.org/10.1007/s11356-015-5648-3), 2016.

1026 Xu, W., Luo, X. S., Pan, Y. P., Zhang, L., Tang, A. H., Shen, J. L., Zhang, Y., Li, K. H.,  
1027 Wu, Q. H., Yang, D. W., Zhang, Y. Y., Xue, J., Li, W. Q., Li, Q. Q., Tang, L., Lu, S.  
1028 H., Liang, T., Tong, Y. A., Liu, P., Zhang, Q., Xiong, Z. Q., Shi, X. J., Wu, L. H.,  
1029 Shi, W. Q., Tian, K., Zhong, X. H., Shi, K., Tang, Q. Y., Zhang, L. J., Huang, J. L.,  
1030 He, C. E., Kuang, F. H., Zhu, B., Liu, H., Jin, X., Xin, Y. J., Shi, X. K., Du, E. Z.,  
1031 Dore, A. J., Tang, S., Collett Jr., J. L., Goulding, K., Sun, Y. X., Ren, J., Zhang, F.  
1032 S., and Liu, X. J.: Quantifying atmospheric nitrogen deposition through a  
1033 nationwide monitoring network across China, *Atmos. Chem. Phys.*, 15, 12345–  
1034 12360, [https://doi.org/10.5194/acp-15-12345-](https://doi.org/10.5194/acp-15-12345-2015) 2015, 2015

1035 Xu, W., Song, W., Zhang, Y. Y., Liu, X. J., Zhang, L., Zhao, Y. H., Liu, D. Y., Tang, A.  
1036 H., Yang, D. W., Wang, D. D., Wen, Z., Pan, Y. P., Fowler, D., Collett, J. L., Erisman,  
1037 J. W., Goulding, K., Li, Y., and Zhang, F. S.: Air quality improvement in a megacity:  
1038 implications from 2015 Beijing Parade Blue pollution control actions, *Atmos.*  
1039 *Chem. Phys.*, 17, 31-46, <https://doi.org/10.5194/acp-17-31-2017>, 2017.

1040 Xu, W., Liu, L., Cheng, M.M., Zhao, Y.H., Zhang, L., Pan, Y.P., Zhang, X.M., Gu, B.J.,  
1041 Li, Y., Zhang, X.Y., Shen, J.L., Lu, L., Luo, X.S., Zhao, Y., Feng, Z.Z., Collett Jr.,  
1042 J.L., Zhang, F.S., and Liu, X.J.: Spatial-temporal patterns of inorganic nitrogen air  
1043 concentrations and deposition in eastern China. *Atmos. Chem. Phys.* 18, 10931–

1044 10954, <https://doi.org/10.5194/acp-18-10931-2018>, 2018.

1045 Xue, T., Liu, J., Zhang, Q., Geng, G.N., Zheng, Y.X., Tong, D., Liu, Z., Guan, D.B., Bo,  
1046 Y., Zhu, T., He, K.B., and Hao, J.M.: Rapid improvement of PM<sub>2.5</sub> pollution and  
1047 associated health benefits in China during 2013–2017, *Sci. China Earth Sci.*, 62,  
1048 1847-1856, <https://doi.org/10.1007/s11430-018-9348-2>, 2019.

1049 Yang, F., Tan, J., Zhao, Q., Du, Z., He, K., Ma, Y., Duan, F., Chen, G., and Zhao, Q.:  
1050 Characteristics of PM<sub>2.5</sub> speciation in representative megacities and across China.  
1051 *Atmos. Chem. Phys.*, 11, 5207-5219, <https://doi.org/10.5194/acp-11-5207-2011>,  
1052 2011.

1053 Ying, H., Yin, Y. L., Zheng, H. F., Wang, Y. C., Zhang, Q. S., Xue, Y. F., Stefanovski,  
1054 D., Cui, Z. L., and Dou, Z. X.: Newer and select maize, wheat, and rice varieties  
1055 can help mitigate N footprint while producing more grain, *Glob. Change. Biol.*, 12,  
1056 4273-4281, <https://doi.org/10.1111/gcb.14798>, 2019.

1057 Yu, S.C., Dennis, R., Roselle, S., Nenes, A., Walker, J., Eder, B., Schere, K., Swall, J.,  
1058 and Robarge, W.: An assessment of the ability of three-dimensional air quality  
1059 models with current thermodynamic equilibrium models to predict aerosol NO<sub>3</sub><sup>-</sup>, *J*  
1060 *Geophys Res-Atmos.*, 110(D7). <https://doi.org/10.1029/2004JD004718>, 2005.

1061 Yue, H. B., He, C. Y., Huang, Q. X., Yin, D., and Bryan, B. A.: Stronger policy required  
1062 to substantially reduce deaths from PM<sub>2.5</sub> pollution in China, *Nat. Commun.*, 11,  
1063 1462, <https://doi.org/10.1038/s41467-020-15319-4>, 2020.

1064 Zhai, S., Jacob, D.J., Wang, X., Liu, Z., Wen, T., Shah, V., Li, K., Moch, J.M., Bates,  
1065 K.H., Song, S. and Shen, L.: Control of particulate nitrate air pollution in China, *Nat.*  
1066 *Geosci.*, 14, 389-395. <https://doi.org/10.1038/s41561-021-00726-z>, 2021.

1067 Zhan, X.Y., Adalibieke, W., Cui, X.Q., Winiwarter, W., Reis, S., Zhang, L., Bai, Z.H.,  
1068 Wang, Q.H., Huang, W.C., and Zhou, F.: Improved estimates of ammonia emissions

1069 from global croplands, *Environ. Sci. Technol.*, 55, 1329-1338,  
1070 <https://doi.org/10.1021/acs.est.0c05149>, 2021.

1071 Zhang, L., Jacob, D. J., Knipping, E. M., Kumar, N., Munger, J. W., Carouge, C. C.,  
1072 van Donkelaar, A., Wang, Y. X., and Chen, D: Nitrogen deposition to the United  
1073 States: distribution, sources, and processes, *Atmos. Chem. Phys.*, 12, 4539–4554,  
1074 <https://doi.org/10.5194/acp-12-4539-2012>, 2012.

1075 Zhang, Q., Zheng, Y. X., Tong, D., Shao, M., Wang, S. X., Zhang, Y. H., Xu, X. D.,  
1076 Wang, J. N., He, H., Liu, W. Q., Ding, Y. H., Lei, Y., Li, J. H., Wang, Z. F., Zhang,  
1077 X. Y., Wang, Y. S., Cheng, J., Liu, Y., Shi, Q. R., Yan, L., Geng, G. N., Hong, C. P.,  
1078 Li, M., Liu, F., Zheng, B., Cao, J. J., Ding, A. J., Gao, J., Fu, Q. Y., Huo, J. T., Liu,  
1079 B. X., Liu, Z. R., Yang, F. M., He, K. B., and Hao, J. M.: Drivers of improved PM<sub>2.5</sub>  
1080 air quality in China from 2013 to 2017, *Proc. Natl. Acad. Sci. U. S. A.*, 49, 24463-  
1081 24469, <https://doi.org/10.1073/pnas.1907956116>, 2019.

1082 Zhang, X. M., Gu, B. J., van Grinsven, H., Lam, S.K., Liang, X., Bai, M., and Chen,  
1083 D.L.: Societal benefits of halving agricultural ammonia emissions in China far  
1084 exceed the abatement costs. *Nat. Commun.*, 11, 4357,  
1085 <https://doi.org/10.1038/s41467-020-18196-z>, 2020a.

1086 Zhang, Y., Vu, T. V., Sun, J., He, J., Shen, X., Lin, W., Zhang, X., Zhang, J., Gao, W.,  
1087 Wang, Y., Fu, T., Ma, Y., Li, W., and Shi, Z.: Significant changes in chemistry of  
1088 fine particles in wintertime Beijing from 2007 to 2017: Impact of clean air actions,  
1089 *Environ. Sci. Technol.*, 54, 1344-1352, <https://doi.org/10.1021/acs.est.9b04678>,  
1090 2020b.

1091 Zhang, Y., Chen, X., Yu, S., Wang, L., Li, Z., Li, M., Liu, W., Li, P., Rosenfeld, D., and  
1092 Seinfeld, J. H: City-level air quality improvement in the Beijing-Tianjin-Hebei



1093 region from 2016/17 to 2017/18 heating seasons: Attributions and process analysis,  
1094 Environ. Pollut., 274, <https://doi.org/10.1016/j.envpol.2021.116523>, 2021a.

1095 Zhang, Y., Liu, X., Zhang, L., Tang, A., Goulding, K., and Collett Jr, J.L.: Evolution of  
1096 secondary inorganic aerosols amidst improving PM<sub>2.5</sub> air quality in the North China  
1097 Plain, Environ. Pollut., 281, 117027,  
1098 <https://doi.org/10.1016/j.envpol.2021.117027>, 2021b.

1099 Zheng, B., Tong, D., Li, M., Hong, C. P., Geng, G. N., Li, H. Y., Li, X., Peng, L. Q.,  
1100 Qi, J., Yan, L., Zhang, Y. X., Zhao, H. Y., Zheng, Y. X., He, K. B., and Zhang, Q.:  
1101 Trends in China's anthropogenic emissions since 2010 as the consequence of clean  
1102 air actions, Atmos. Chem. Phys., 18, 14095-14111, [https://doi.org/10.5194/acp-18-](https://doi.org/10.5194/acp-18-14095-2018)  
1103 [14095-2018](https://doi.org/10.5194/acp-18-14095-2018), 2018.

1104 Zheng, G. J., Duan, F. K., Su, H., Ma, Y. L., Cheng, Y., Zheng, B., Zhang, Q., Huang,  
1105 T., Kimoto, T., Chang, D., Pöschl, U., Cheng, Y. F., and He, K. B.: Exploring the  
1106 severe winter haze in Beijing: the impact of synoptic weather, regional transport  
1107 and heterogeneous reactions, Atmos. Chem. Phys., 15, 2969–2983,  
1108 <https://doi.org/10.5194/acp-15-2969-2015>, 2015.